Article

Developmental Cell

A Mechanism Coupling Systemic Energy Sensing to Adipokine Secretion

Graphical Abstract

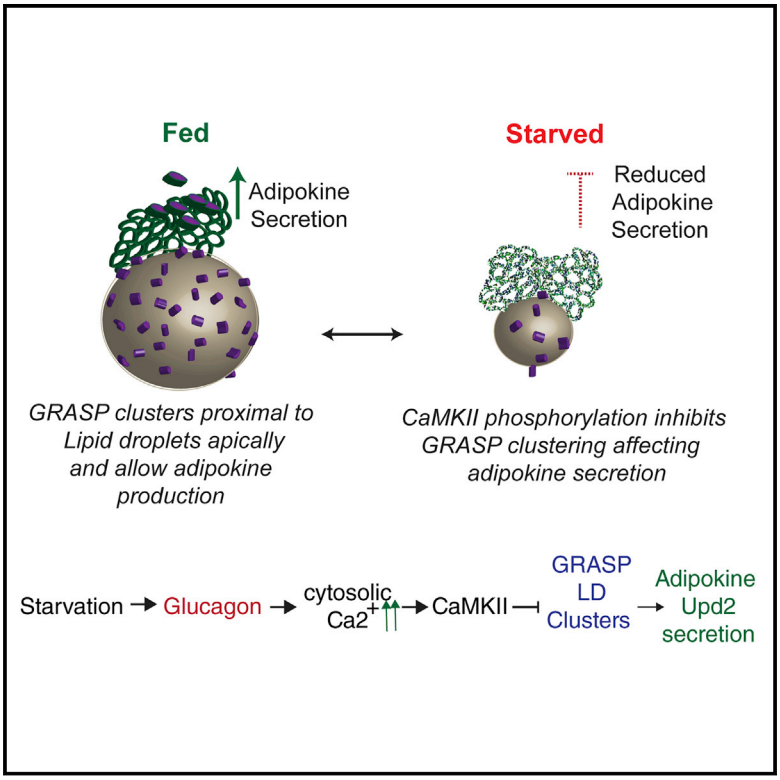

Highlights

- Adipokine Upd2 localizes to GRASP clusters in the proximity of lipid droplets
- Starvation increases GRASP phosphorylation and inhibits its apical clustering
- Glucagon-mediated Ca^{2+} increase triggers CaMKII phosphorylation of GRASP
- Increased cytosolic Ca^{2+} negatively regulates adipokine secretion via GRASP

Authors

Akhila Rajan, Benjamin E. Housden, Frederik Wirtz-Peitz, Laura Holderbaum, Norbert Perrimon

Correspondence

akhila@fredhutch.org (A.R.), perrimon@genetics.med.harvard.edu (N.P.)

In Brief

Rajan et al. identify a mechanism coupling nutrient status to adipocyte-mediated adipokine secretion involving glucagon-mediated calcium signaling and GRASP, an unconventional secretion protein. In fly fat cells, leptin ortholog Upd2 is associated with GRASP near lipid droplets, and, upon nutrient deprivation, increased calcium levels negatively regulate adipokine secretion via GRASP.

Rajan et al., 2017, Developmental Cell *43*, 83–98
October 9, 2017
https://doi.org/10.1016/j.devcel.2017.09.007

CellPress

Developmental Cell
Article

A Mechanism Coupling Systemic Energy Sensing to Adipokine Secretion

Akhila Rajan,[1,6,*] Benjamin E. Housden,[2,4,5] Frederik Wirtz-Peitz,[2,5] Laura Holderbaum,[1] and Norbert Perrimon[2,3,*]
[1]Basic Sciences Division, Fred Hutch, Seattle, WA 98109, USA
[2]Department of Genetics, Harvard Medical School, Boston, MA 02115, USA
[3]Howard Hughes Medical Institute, Chevy Chase, MD 20815, USA
[4]Present address: University of Exeter, Living Systems Institute, Exeter EX4 4QD, UK
[5]These authors contributed equally
[6]Lead Contact
*Correspondence: akhila@fredhutch.org (A.R.), perrimon@genetics.med.harvard.edu (N.P.)
https://doi.org/10.1016/j.devcel.2017.09.007

SUMMARY

Adipocytes sense systemic nutrient status and systemically communicate this information by releasing adipokines. The mechanisms that couple nutritional state to adipokine release are unknown. Here, we investigated how Unpaired 2 (Upd2), a structural and functional ortholog of the primary human adipokine leptin, is released from *Drosophila* fat cells. We find that Golgi reassembly stacking protein (GRASP), an unconventional secretion pathway component, is required for Upd2 secretion. In nutrient-rich fat cells, GRASP clusters in close proximity to the apical side of lipid droplets (LDs). During nutrient deprivation, glucagon-mediated increase in calcium (Ca^{2+}) levels, via calmodulin kinase II (CaMKII) phosphorylation, inhibits proximal GRASP localization to LDs. Using a heterologous cell system, we show that human leptin secretion is also regulated by Ca^{2+} and CaMKII. In summary, we describe a mechanism by which increased cytosolic Ca^{2+} negatively regulates adipokine secretion and have uncovered an evolutionarily conserved molecular link between intracellular Ca^{2+} levels and energy homeostasis.

INTRODUCTION

Energy homeostasis is the ability of organisms to sense nutrient flux, and alter both physiology and behavior, enabling the maintenance of certain physiological parameters, such as blood glucose and fat stores, within a permissible range. Dysfunctional energy homeostasis underlies a number of chronic health disorders, in particular, obesity, anorexia, and diabetes. Reliable systemic communication of energy stores is key to ensuring robust energy homeostasis.

Adipose tissue, composed of adipocytes, is an endocrine organ whose primary role is energy storage. A significant portion of energy stores is comprised of the neutral lipid triacylglycerol (TAG), contained in a specialized intracellular organelles termed lipid droplets (LDs) (Walther and Farese, 2012).

A key property of adipocytes is their dynamic response to an organism's systemic energy state. Under a positive nutritional state, lipids are stored as TAG, and in low-energy states TAG is mobilized to generate free fatty acids (Duncan et al., 2007), which fuel the organism. This dynamic regulation is made possible by the ability of adipocytes to respond to anabolic hormones such as insulin and catabolic hormones such as glucagon, which promote lipogenesis and lipolysis, respectively.

Adipocytes not only respond to insulin and glucagon but also communicate their stored energy reserves systemically by secreting proteins, referred to as adipokines (Trayhurn and Beattie, 2001). These include cytokines such as tumor necrosis factor alpha and adiponectin (Scherer et al., 1995), which act in other peripheral tissues to regulate energy metabolism, and the peptide hormone leptin (Zhang et al., 1994), which impinges on central brain circuits to regulate appetite and energy expenditure (Flak and Myers, 2015; Morton et al., 2006). Thus, energy homeostasis is maintained by a complex interplay between hormonal systems, with adipocytes playing an integral role in both sensing systemic nutritional state, and by communicating total energy stores to the organism. Mutations of leptin or its receptor are associated with severe obesity in humans (Farooqi and O'Rahilly, 2009; Montague et al., 1997), highlighting the key role played by this signaling axis in maintenance of energy homeostasis. Leptin production in response to total stored energy is regulated at the level of both translation and secretion (Barr et al., 1997b; Fried et al., 2000; Lee and Fried, 2006; Lee et al., 2007). However, the molecular mechanisms underlying how energy sensing is coupled to leptin secretion are poorly understood (Dugail and Hajduch, 2007).

In *Drosophila*, the functional ortholog of leptin are the Unpaired cytokines (Upd1 and Upd2). While neuronal-derived Upd1 regulates feeding behavior by inhibiting the food-seeking neuropeptide-Y circuit (Beshel et al., 2017), Upd2 is a secreted factor produced from the fat body in response to dietary fat and sugars (Rajan and Perrimon, 2012). The physiological roles of Upd2 and leptin are similar in the context of response to nutrient deprivation and energy sensing. For example, both Upd2 and leptin are upregulated by increased fat stores, and downregulated by reduced systemic nutrient levels. In mice, leptin downregulation during starvation is required for increasing survival capacity of the organism under adverse nutrient conditions (Ahima et al., 1996). Consistent with this, *upd2* mutants are starvation resistant

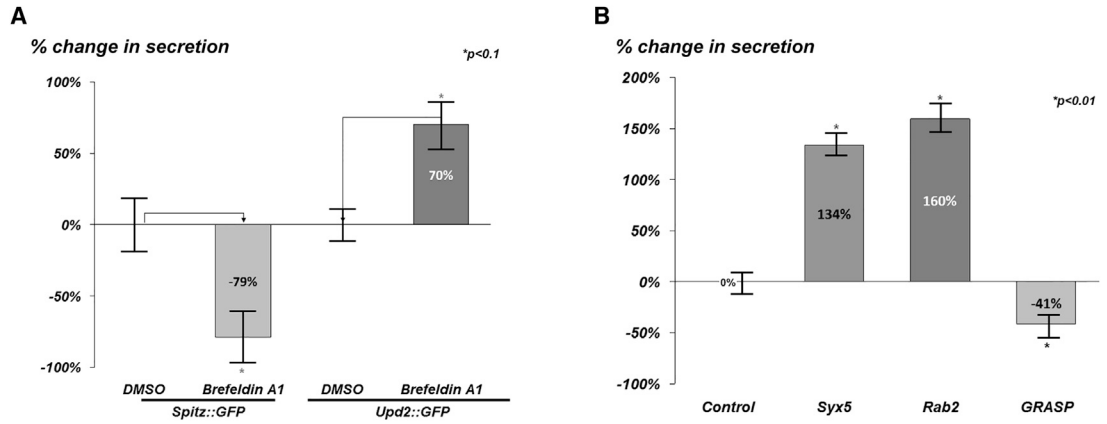

Figure 1. *Drosophila* Upd2 Adopts an Unconventional Secretion Route Mediated by GRASP

(A) Quantification of normalized fold change in secreted GFP signal detected by GFP sandwich ELISA assay performed on conditioned medium of S2R+ cells. Cells were transfected with *spitz::GFP* and *Upd2::GFP*, and treated with Brefeldin A1 (17.85 μM) or DMSO (control) for 18 hr.

(B) Normalized fold change of secreted Upd2::GFP assayed by GFP sandwich ELISA assay from conditioned media of S2R+ transfected cells treated with Upd2::GFP and dsRNAs (dsRNA *LacZ* [control] or dsRNAs targeting *syntaxin-5*, *Rab2*, and *GRASP*).

Error bars represent %SD. Statistical significance quantified by t test on six biological replicates per condition. *p < 0.1 in (A) and *p < 0.01 in (B). See also Figure S1.

(Rajan and Perrimon, 2012). Hence, the ancestral role of leptin and Upd2 likely arose from the need to remotely signal systemic nutrient status (Flier and Maratos-Flier, 2017). This functional conservation, along with the genetic tractability of *Drosophila*, makes this an ideal system in which to study the mechanisms linking energy store sensing and adipokine secretion.

Our studies, in *Drosophila* adult fat body cells, reveal that Upd2 is secreted via a Golgi bypass mechanism mediated by Golgi reassembly stacking protein (GRASP), a component involved in non-conventional protein secretion (Kinseth et al., 2007). *GRASP* mutants display systemic energy storage defects that resemble loss of Upd2, consistent with the role of GRASP in Upd2 secretion. Importantly, we find that GRASP apico-basal localization and phosphorylation is sensitive to nutrient state, and regulated by adipokinetic hormone (AKH), the *Drosophila* functional analog of glucagon (Kim and Rulifson, 2004). Increased cytosolic Ca^{2+} concentrations and Ca^{2+} sensing calmodulin kinase II (CaMKII) activity reduce Upd2 secretion. Thus, we have uncovered a molecular link showing how the second messenger Ca^{2+} negatively regulates adipokine secretion in *Drosophila* fat cells.

RESULTS

Upd2 Is Secreted by an Unconventional Secretion Pathway Mediated by GRASP

To investigate how Upd2 secretion is regulated by nutrients, we set out to identify which secretory route is required for Upd2 production. We used *Drosophila* S2R+ cells which have been used previously to characterize genes involved in secretion (Bard et al., 2006; Kondylis et al., 2011), JAK/STAT signaling (Baeg et al., 2005), and LD biology (Guo et al., 2008). Specifically, we assayed GFP-tagged Upd2 secretion (*upd2::GFP*), which is functional and capable of activating the STAT receptor (Hombria et al., 2005; Rajan and Perrimon, 2012; Wright et al., 2011).

Most secreted proteins are transported from the endoplasmic reticulum (ER) to the Golgi. We used three different assays in S2R+ cells to determine whether Golgi function was required for Upd2 secretion. We treated cells with the fungal toxin Brefeldin A1 (BFA), which disrupts Golgi recruitment (Lippincott-Schwartz et al., 1989). Upd2 was detectable in the media from S2R+ cells treated with BFA (Figure 1A), whereas the positive control Spitz, an epidermal growth factor-like ligand whose trafficking via Golgi is required for its secretion (Lee et al., 2001), was detected at reduced levels (79% reduction) in the media. Next, we tested whether Upd2 secretion was sensitive to Endoglycosidase H (Endo H) (Maley et al., 1989), which removes specific N-linked glycans added in the ER. Proteins that pass through the Golgi acquire resistance to Endo H due to glycans added only in the Golgi. Upd2 was sensitive to Endo H, as shown by a mobility shift in PAGE (Figure S1), suggesting that it is not secreted by the conventional Golgi pathway. Finally, we asked whether Upd2 secretion was dependent on the intra-Golgi SNARE proteins Syntaxin5 (Dascher et al., 1994) and Rab2 (Friggi-Grelin et al., 2006), which are both required for anterograde transport from the Golgi. Strikingly, Upd2 secretion was not impaired in cells with either Syntaxin5 or Rab2 knockdown (Figure 1B). Also, unexpectedly, Upd2 secretion is significantly upregulated when Golgi-based anterograde transport is inhibited by BFA treatment (Figure 1A) or genetic disruption of anterograde transport (Figure 1B). Such an observation has been reported for proteins which adopt a non-traditional secretion route (Tveit et al., 2009). Taken together, these data suggest that Upd2 secretion bypasses the Golgi and instead depends on the unconventional secretion pathway. Hence, we examined if Upd2 requires GRASP, an evolutionarily conserved protein that mediates unconventional secretion in organisms ranging from ameba to humans (Dupont et al., 2011; Gee et al., 2011; Kinseth et al., 2007; Manjithaya et al., 2010; Schotman et al., 2008). While there are two forms of GRASP in mammals, *GRASP55* and *GRASP65, Drosophila* has a single ortholog *dGRASP,* which

we refer to as *GRASP*. We observed that dsRNAs against *GRASP* cause significant reduction in Upd2 secretion (Figure 1B), strongly suggesting that GRASP is required for Upd2 secretion by the unconventional route.

Drosophila GRASP, via Its Role in Upd2 Secretion, Affects Systemic Lipid Homeostasis

To further examine the relationship between GRASP and Upd2, we generated a *GRASP* mutant, *GRASP-del*, using the CRISPR/Cas9 technology (see STAR Methods and Figure S2A). *GRASP-del* homozygous mutant flies do not produce GRASP protein (Figure S2B) and are viable and fertile, although they exhibit a slight developmental delay.

The requirement for GRASP in Upd2 secretion in S2R+ cells led us to test the physiological role of GRASP in energy balance. The primary metabolic phenotype of Upd2 is a significant reduction in stored fat, i.e., TAG levels. Hence, we assayed relative normalized TAG levels in *GRASP-del* mutants compared with a background matched control. As predicted, homozygous *GRASP-del* and *trans*-heterozygous *GRASP/Deficiency* animals show a significant reduction in TAG levels (Figure 2A), reminiscent of the reduction in energy stores observed in *upd2* mutants (Rajan and Perrimon, 2012).

Removal of *upd2* specifically in fat cells is sufficient to reduce fat stores, while its removal in other tissues, such as the muscle, has no effect on energy stores (Rajan and Perrimon, 2012). Therefore, we next asked whether the role of GRASP in maintaining energy balance is also fat tissue specific and phenocopies *upd2*. Knockdown of *GRASP* specifically in fat cells, using three independent *GRASP-RNAi* lines, significantly reduced TAG levels, whereas knockdown of *GRASP* in muscles (*Mhc-Gal4>GRASP-i*) did not affect fat storage (Figure S2C). These data suggest that GRASP plays a fat cell-specific role in the maintenance of lipid stores, a phenotype consistent with a role in mediating Upd2 secretion.

To establish a fat cell-specific role of GRASP in maintaining lipid stores, we determined whether the TAG storage defect in *GRASP-del* homozygous mutants (Figure 2A) could be rescued by fat tissue-specific expression of GRASP. We generated flies that expressed a GFP-tagged *GRASP* transgene (*UAS-GRASP::GFP*) only in fat cells of *GRASP-del* mutant flies. This was sufficient to rescue the fat storage defect of *GRASP-del* mutants (Figure 2C), strongly suggesting that GRASP regulates fat stores primarily via its activity in fat cells. Note the variability in *GRASP-del* fat storage levels between the two datasets (Figures 2A and 2C). This is an age-dependent effect of the fat storage phenotype in *GRASP-del* mutants. For initial analysis of *GRASP-del* mutants, fat storage was assessed on day 7 (Figure 2A). As we progressed in our phenotypic characterization, we found that the fold change in TAG stores, for both *Upd2-del* and *GRASP-del*, was more pronounced with age. Hence, we performed the rescue experiments under more stringent conditions by testing TAG storage rescue at a 15 day time point (Figure 2C).

To establish whether GRASP plays a role in Upd2-mediated lipid storage, we tested the requirement of GRASP for the increase in stored fat levels associated with Upd2 overexpression (Figure 2D). RNAi-mediated knockdown of *GRASP* suppressed the effect of Upd2 overproduction on fat storage (Figure 2D), strongly suggesting that GRASP function is required for the effect of Upd2 on systemic fat storage.

Similar to how insulin accumulation in insulin-producing cells (IPCs) is used as a readout for circulating insulin levels (Geminard et al., 2009; see Discussion), we tested the level of Upd2 accumulation in fat cells in which *GRASP* levels are reduced by RNAi. Consistent with the hypothesis that GRASP is required for Upd2 secretion *in vivo*, we observed an increase in Upd2 accumulation in *Lpp-Gal4::GRASP-RNAi* fat cells (Figure 2E). Based on this result (Figure 2E), together with the requirement of GRASP for Upd2 to exert its effect on TAG storage (Figure 2D), and the Upd2 secretion defect upon GRASP removal in S2R+ cells (Figure 1C), we conclude that GRASP mediates Upd2 secretion in *Drosophila* fat cells.

Upd2 remotely controls insulin secretion from IPCs in the fly brain (Rajan and Perrimon, 2012). Therefore, we assayed whether the defects in fat storage in *GRASP* mutants result from impaired insulin secretion. We quantified insulin accumulation in IPCs when *GRASP* was specifically removed from fat cells (*Lpp-Gal4>GRASP-RNAi*), and observed a significant increase in insulin accumulation from two independent RNAi lines (Figure 2F). In addition, GRASP removal from IPCs themselves did not have an impact on insulin accumulation, suggesting that GRASP plays a non-autonomous role in regulating insulin release (Figure S2F).

To test whether the insulin secretion defect is the primary cause of the lipid storage defects in *GRASP* mutants, we generated flies in which the IPCs remain depolarized (*Dilp-Gal4>UAS-TrpA1*) in a *GRASP-del* mutant background. Strikingly, IPC depolarization resulted in constitutive insulin release, which was sufficient to rescue the fat storage defects of *GRASP-del* flies (Figure 2G). In addition to fat storage defects, both insulin (Dilp) deletion flies and *upd2* null mutants show starvation resistance (Rajan and Perrimon, 2012; Zhang et al., 2009). *GRASP-del* flies also display a starvation resistance phenotype (Figure S2D). In addition, GRASP does not have a cell-autonomous role in the IPCs with respect to fat storage, as IPC-specific *GRASP* knockdown (*Dilp2-Gal4> UAS-GRASP-RNAi*) did not cause any fat storage defects (Figure S2E). Altogether, these results suggest that GRASP is required for Upd2-mediated insulin release. Our observations are consistent with a model where GRASP plays a role in Upd2 secretion from fat tissue, which in turn impinges on remote regulation of insulin release from the brain, thus regulating systemic lipid homeostasis.

GRASP Phosphorylation in *Drosophila* Adult Fat Cells Is Nutrient Sensitive and Regulated by CaMKII

Given the involvement of GRASP in Upd2 secretion, a protein which signals systemic nutrient state, we tested whether GRASP itself, similar to Upd2 is regulated in a nutrient-sensitive manner. Prior work on GRASP regulation during mitosis revealed that a primary mode of GRASP regulation is its phosphorylation by mitotic kinases such as Cdc2 and polo kinase (Wang et al., 2005; Yoshimura et al., 2005). Hence, we speculated that the GRASP phosphorylation state could be contingent on systemic nutrient status, regulated by nutrient-sensitive kinases. To test this, we expressed the 92 kDa GFP-tagged GRASP in *Drosophila* adult fat cells and assessed its phosphorylation status using

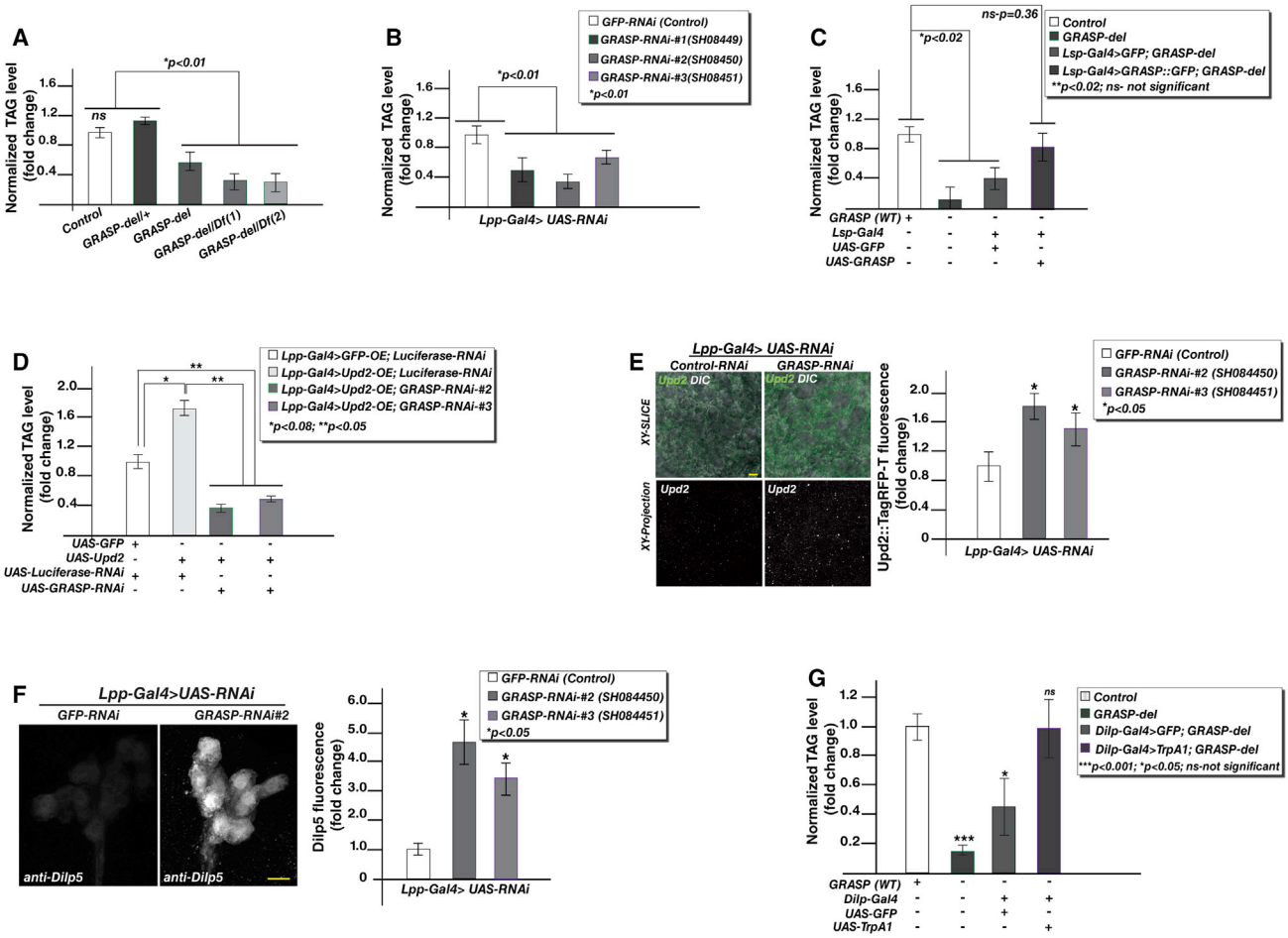

Figure 2. *Drosophila* GRASP, via Its Role in Upd2 Secretion, Affects Systemic Lipid Homeostasis

(A–D) Normalized triacylglycerol (TAG) levels in adult *Drosophila* males relative to controls. (A) Control (Cas9/CRISPR background strain) compared with heterozygous *GRASP* deletion strain (*GRASP-del*/+), homozygous *GRASP* deletion (*GRASP-del*), and *trans*-heterozygotes *GRASP* deletion (*GRASP-del*/*Df*). The two deficiencies, *Df(3L)BSC552* and *Df(3L)BSC445,* uncover the cytological region of *GRASP*. (B) Fat cell-specific *GRASP* knockdown, using three independent transgenic strains (*GRASP-RNAi*), compared with control (*GFP-RNAi*). (C) Fat cell-specific overexpression of GFP-tagged GRASP (*GRASP::GFP*) and control transgene (*GFP*) in *GRASP* deletion (*GRASP-del*) background, relative to triglyceride levels of control (Cas9/CRISPR background strain).

(D) Effect of fat cell-specific Upd2 overexpression (*UAS-Upd2*) relative to GFP overexpression (*UAS-GFP*) in *GRASP* knockdown strains (*GRASP-RNAi*), compared with control (*Luciferase-RNAi*).

(E) Confocal images showing single optical section (xy slice) and projection of numerous optical slices (xy projection) of *Drosophila* adult fat cells expressing of Upd2::tagRFP-T (green). To identify the difference between *GRASP* knockdowns (*GRASP-RNAi*) versus control (*GFP-RNAi*), accumulation of Upd2 (green) in fat cells is assayed by confocal image analysis. Quantification of total Upd2 signal in fat cells shows a significant increase in Upd2 signal in *GRASP* knockdown. Scale bar, 5 μm.

(F) Projection of optical xy sections of insulin-producing cells (IPCs) in the *Drosophila* adult brain stained with an antibody against *Drosophila* insulin (*Dilp5*) in control (*Lpp-Gal4> UAS-GFP-RNAi* background) and fat-specific *GRASP* knockdown (*Lpp-Gal4>UAS-GRASP-RNAi*). Quantification of the relative change in total Dilp5 fluorescence in IPC bodies from images acquired under the same conditions from control and two independent transgenic strains (*GRASP-RNAi*). Scale bar, 10 μm.

(G) Quantification of normalized TAG levels in flies that have insulin neuron-specific expression of a control transgene (*GFP*), or transgene that activates neurons (*TrpA1*) in *GRASP-del* background, relative to control (Cas9/CRISPR background strain).

Error bars represent the percentage SD. Statistical significance quantified by t test on three to six biological replicates per condition for TAG assays, and seven to ten animals for image acquisition experiments. The p values for each experiment are indicated in graphs. See also Figure S2.

phosphoprotein stains and western blots of lysates from fed and starved states. In three independent experiments, under starvation conditions, GRASP protein levels slightly decreased, and GRASP phosphorylation increased (Figures 3A, S3A, S3B, and S3D). Note that for this analysis we used a tagged form of GRASP, *UAS-GRASP::GFP* that can rescue the metabolic phenotypes of *GRASP-del* (Figure 2C), as it permits us to probe GRASP phosphorylation status during systemic nutritional change in a tissue-specific manner. In addition, we focused our analysis in fat tissues because removal of GRASP in other cells and tissues did not impact energy physiology (Figures S2C and S2E). Altogether, our observations (Figures 3A, S3A, and S3B) suggest that GRASP protein levels and phosphorylation are regulated by systemic nutrient state in fat tissues.

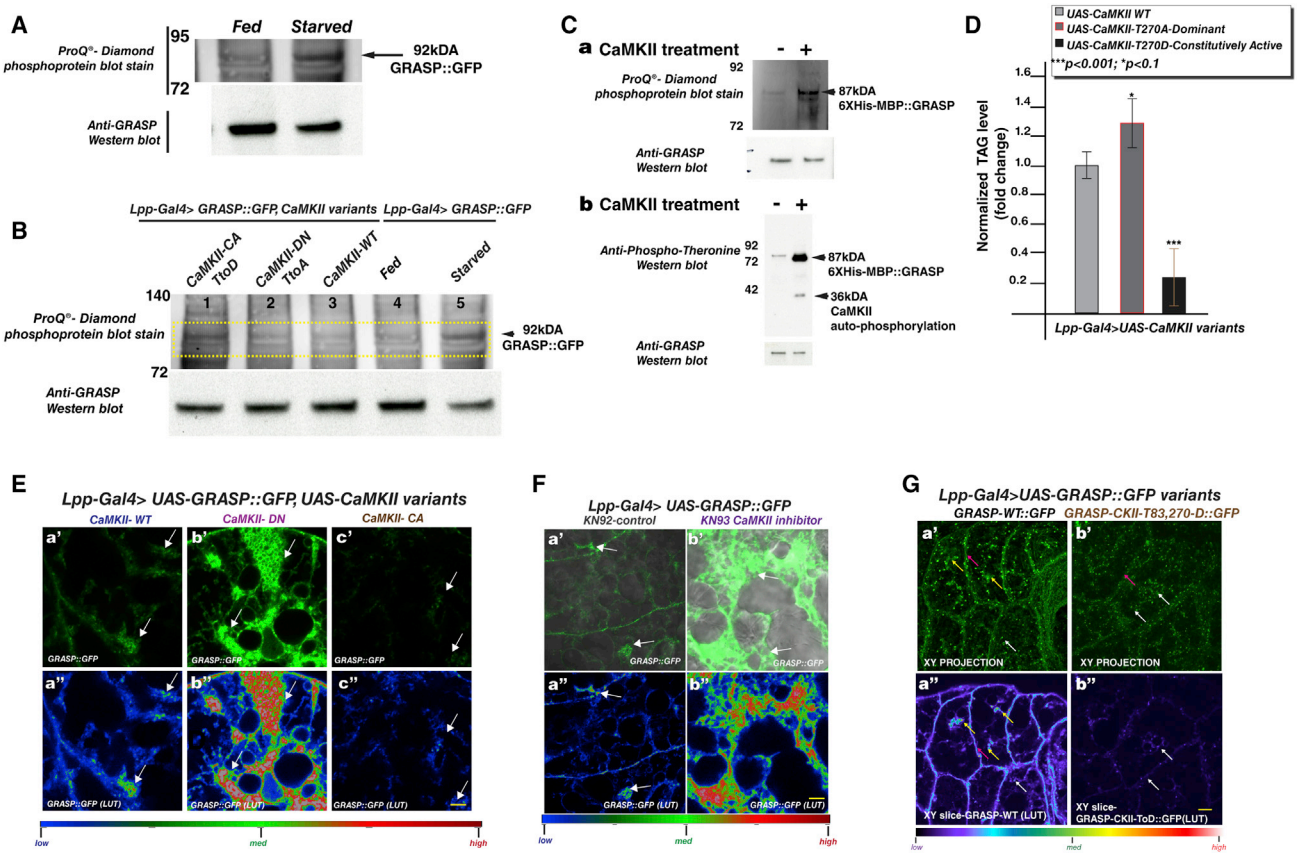

Figure 3. GRASP Phosphorylation in *Drosophila* Adult Fat Cells Is Nutrient Sensitive and Regulated by CaMKII

(A) Protein lysates from flies expressing GFP-tagged GRASP specifically in fat cells; 25 μg of protein was loaded per lane from flies subjected to starvation versus those fed *ad libitum*. The western blot was stained with ProQ-Diamond phosphoprotein stain and laser scanned (see the STAR Methods) to identify protein bands that specifically fluoresce when phosphoproteins are present. Compare the change in the 92 kDa GRASP band between fed and starved states. The same blot is probed with anti-GRASP antibody, which recognizes the GRASP::GFP band at 92 kDa. See Figure S3A for control ProQ-Diamond phosphoprotein stain and anti-GRASP blots with lysates treated with lambda phosphatase.

(B) *In vivo* test to assay the effect of CaMKII on GRASP phosphorylation in fat cells; 25 μg of protein lysates from flies expressing GFP-tagged GRASP in fat tissue together with different *CaMKII* transgenes (CaMKII constitutively active [*CaMKII-CA TtoD*, lane 1], CaMKII dominant negative [*CaMKII-DN TtoA*, lane 2], and CaMKII wild-type [*CaMKII-WT*, lane 3]) were western blotted and stained with ProQ-Diamond phosphoprotein stain (see the STAR Methods). In addition, lysates from GRASP::GFP expressing flies, subject to *ad libitum* feeding (lane 4) or starvation (lane 5), were probed for altered phosphorylation using ProQ-Diamond phosphoprotein stain. Note that lysates from CaMKII constitutive activation (lane 1) showed increased phosphorylation signature, similar to starved flies (lane 5). The same blot was probed with anti-GRASP antibodies. Note that the total GRASP level remains unaltered in the context of CaMKII activation (lane 1) or inhibition (lane 2), compared with control (lane 3), whereas a slight reduction in GRASP levels was observed during starvation (lane 5). See Figure S3D for control *MemCode* total protein stain and anti-Lsp1-gamma blots serving as loading control of another fat protein.

(C) *In vitro* kinase assay of *Drosophila* GRASP (6XHis-MBP::GRASP) incubated with CaMKII (see the STAR Methods). The mock control (–) and experimental (+) reactions were probed for changes in phosphorylation using ProQ-Diamond phosphoprotein stain (a) and with an anti-phosphothreonine antibody (b). A significant increase in phosphorylation is detected when GRASP is incubated with CaMKII. Blots were probed with anti-GRASP antibody to test for equal loading. Note that the CaMKII auto-phosphorylation band is detected with anti-phosphothreonine (b).

(D) Quantification of normalized TAG levels in flies with fat cell-specific expression of CaMKII variant transgenes. Note the significant reduction in stored fat when the CaMKII constitutively active form is expressed (*CaMKII-CA*). The p values are based on two-tailed t test, and error bars represent %SD. Three biological replicates were used per data point.

(E) Representative images at an apical section of adult fat tissue from flies expressing GFP-tagged GRASP together with different CaMKII transgenes - CaMKII wild-type (*CaMKII-WT*–, a′ and a″), CaMKII dominant negative (*CaMKII-DN*, b′ and b″), and CaMKII constitutively active (*CaMKII-CA*, c′ and c″). White arrows point to GRASP clustered apical localization. The intensity of GRASP is represented in a″–c″ (see look up table [LUT]). Note that acute CaMKII inhibition results in a significant increase of GRASP apical localization (b′ and b″) compared with control (a′ and a″). GRASP apical localization is undetectable in the context of CaMKII constitutive activation (c′ and c″).

(F) *Ex vivo* assay to test the effect of acute CaMKII inhibition on GRASP hub formation. Confocal images captured at an apical plane from fat explants of flies expressing GFP-tagged GRASP in fat tissues. Explants were cultured for 15 min prior to imaging with control drug (inactive CaMKII inhibitor KN92 [a′ and a″]) or with CaMKII inhibitor (b′ and b″, KN93). Note the striking expansion of GRASP apical localization (white arrows) at the lipid droplet (LD) periphery in the context of acute CaMKII inhibition. The intensity of GRASP is represented in a″ and b″ (see LUT).

(G) *Drosophila* fat cells expressing GFP-tagged GRASP WT (a′ and a″) and putative phosphomimetic for CaMKII GRASP (b′ and b″). (a′ and b′) XY projections of all planes through a confocal z stack. (a″ and b″) The mean gray values of GRASP::GFP in the entire z stack of fat tissue in both WT (a′) and phosphomimetic (b′) in a

(legend continued on next page)

To identify which proteins interact with GRASP in a nutrient-dependent manner, we performed label-free semi-quantitative mass spectrometry (MS) on GRASP immunoprecipitated (IP) from adult *Drosophila* fat tissues obtained from flies which were fed *ad libitum* or starved (Figure S3B). We analyzed MS datasets from four independent IP-MS experiments, done in triplicate, to identify interactors. Two kinases, the intracellular calcium (Ca^{2+} sensing kinase CaMKII) (Figure S3C) and diacylglycerol sensing kinase protein kinase C-D, had differential spectral counts between fed and starved states. We focused on CaMKII because we recovered a number of Ca^{2+} sensing and binding proteins as GRASP interactors (Figure S3C).

We assayed the effect of CaMKII on GRASP phosphorylation *in vivo* in fat cells and engineered flies expressing wild-type (WT), constitutively active (CA), and dominant negative (DN) forms of *CaMKII* (Koh et al., 1999) in fat cells that also expressed GFP-tagged GRASP. Note that, since constitutive expression of these transgenes in fat cells produced lethality, we expressed them using the *tubGal80ts* system from days 5 to 10 and then assayed the effect on GRASP. Protein lysates were probed for alterations in the phosphorylation state of the 92 kDa GRASP::GFP band (Figure 3B, lanes 1–3). For comparison with altered systemic nutrient state, we also prepared protein lysates from GFP-tagged GRASP expressing flies that were fed *ad libitum* or starved (Figure 3B, lanes 4, 5). We observed increased phosphoprotein staining of the GRASP::GFP band from flies expressing CA CaMKII (Figure 3B, lane 1), which is comparable with the increased phosphoprotein stain observed in the starved state (Figure 3B, lane 5). The same blot was probed with anti-GRASP. Whereas starvation affects both GRASP protein level and its phosphorylation state (Figures 3A and 3B, lanes 4, 5), the GRASP::GFP protein levels in all three CaMKII transgenes were comparable (Figure 3B, lanes 1–3). This suggests that CaMKII activation or inhibition does not change total GRASP::GFP protein levels but only the GRASP phosphorylation state (see also companion Figure S3D for loading controls).

We confirmed that *Drosophila* GRASP is a CaMKII substrate by performing *in vitro* kinase assays using recombinant *Drosophila* GRASP incubated with activated CaMKII. The reaction product, after western blotting using both phosphoprotein staining (Figure 3Ca) and anti-phosphothreonine (Figure 3Cb), revealed a strong phosphorylation signature only in the experimental incubation (Figure 3C). Taken together, these data suggest that GRASP is a target of CaMKII in *Drosophila* fat cells, and that phosphorylation by CaMKII does not increase or decrease GRASP protein levels.

Given that GRASP is a CaMKII target (Figures 3B and 3C), and that lack of *GRASP* activity in fat cells results in reduced stored fat levels (Figures 2A and 2B), we investigated whether genetically altering CaMKII activity in fat cells had an impact on TAG levels. Thus, we compared the levels of fat when *CaMKII-DN* or *CaMKII-CA* transgenes were expressed in fat tissue with the *CaMKII-WT* control (Koh et al., 1999). Activation of CaMKII significantly reduced fat stores (Figure 3D). While this is likely due to its effect on numerous downstream targets, it resembles the effect on fat stores in a starved state as well as phenocopies loss of *GRASP* or *upd2*.

Next, we expressed WT, CA, or DN forms of *CaMKII* (Figure 3E) and examined how GRASP::GFP expression in fat tissues was affected. We imaged tissues under the same conditions and at the same depth from apical surfaces (4 μM). The expression of *CaMKII-DN* caused a significant increase in GRASP intensity (Figures 3Eb′ and 3Eb″) compared with WT control (Figures 3Ea′ and 3Ea″, see look up table), while constitutive activation of *CaMKII-CA* was associated with decreased GRASP intensity (Figures 3Ec′ and 3Ec″). However, as phosphorylation by CaMKII does not increase or decrease GRASP protein levels (Figure 3B, lanes 1–3), and that molecular brightness analysis of EGFP-tagged proteins has been used as a measure of aggregation state of proteins, such as nuclear receptors (Chen et al., 2003), it suggests that alterations in GRASP intensity represent the extent of GRASP oligomerization in response to phosphorylation by CaMKII. This observation is reminiscent of the role of phosphorylation by other kinases that regulate GRASP oligomerization during mitosis (Wang et al., 2005; Yoshimura et al., 2005).

To further test whether CaMKII acutely regulates GRASP clustering, we performed a CaMKII inhibition *ex vivo* assay in which we cultured adult fly fat tissue explants expressing GFP-tagged GRASP in the presence of the CaMKII inhibitor KN93 briefly (15 min) and imaged fat tissues. CaMKII inhibition within 15 min significantly increased GRASP intensity (Figure 3Fb′). Given the brief period in which we observe this effect, it is unlikely to be a result of increased GRASP protein production, but instead clustering of GRASP, which produces a brighter intensity signal (Chen et al., 2003). This model is consistent with our observations that manipulating CaMKII does not affect GRASP protein levels but only its phosphorylation status (Figure 3B).

CaMKII has potentially two phosphorylation motifs (RXXS/T) on *Drosophila* GRASP. This motif is also conserved in human GRASP55 protein (T83 and T270, see sequence alignment Figure S3E). We generated GRASP::GFP transgenic flies in which these two putative phosphorylation sites are mutated

sample set of four animals per genotype is comparable. Average mean gray value: WT (a′) = 23.6 and phosphomimetic (b′) = 20.7 (p value in two-tailed t test = 0.38, indicating not a significant difference). This is consistent with the observation that CaMKII overactivation does not alter GRASP protein level, compare (B) lane 1 and lane 3. These data indicate that CaMKII-mediated phosphorylation affects the ability of GRASP to exhibit a clustered localization at LD and membrane. Single XY slice images of confocal micrographs acquired at an approximate depth of 3.5 μM from the apical surface of fat cells expressing GFP-tagged GRASP WT (a″) and putative phosphomimetic GRASP (b″). Yellow arrows point to LD-associated GRASP clusters; pink arrows to membrane associated; white arrows to punctate localization. Note the absence of GRASP membrane and cluster localization in the GRASP putative phosphomimetic versions (b′ and b″). See S3F for a montage view of XY slices through a z stack in order to represent a sample of apical XY slices from 2 to 6 μM. The intensity of GRASP is represented in a″ and b″ (see LUT). Note that the CaMKII phosphomimetic mutant GRASP transgene in (G) b′ and b″, phenocopies GRASP localization in fat tissues when CaMKII is constitutively activated in (E) c′ and c″. See Figure S3E for Clustal W alignment of *Drosophila* GRASP with mammalian GRASP 55 and 65, used for prediction of conserved CaMKII phosphorylation sites.

Scale bars, 5 μm (Figures 3E–3G). See also Figure S3.

(threonine [T] to aspartate [D]) to mimic a constitutively phosphorylated state, i.e., phosphomimetic version. Next, we assayed how these point mutations affect GRASP localization in fat cells. The xy projection of z stacks (Figures 3Ga′ and 3Gb′) and montage of xy slices (Figures S3Fa and S3Fb) show that GRASP phosphomimetic is expressed, but is excluded from clusters and membrane, and largely present in the punctate fraction. The punctate expression of GRASP phosphomimetic version (Figures 3Gb′ and 3Gb″) phenocopies GRASP localization under a CaMKII-CA state (Figures 3Ec′ and 3Ec″). The mean gray values of GRASP:GFP in the entire z stack of fat tissue is comparable between GRASP WT (a′) and GRASP phosphomimetic (b′). Specifically, in a sample set of four animals per genotype, average mean gray values of WT (Figure 3Ga′ = 23.6) and phosphomimetic (Figure 3Gb′ = 20.7) are not significant different (p value in two-tailed t test = 0.38). These data indicate that CaMKII-mediated phosphorylation does not affect GRASP protein levels, but affects GRASP phosphorylation. In summary, in the fly fat, we have strong evidence supporting the model that CaMKII-mediated phosphorylation negatively regulates GRASP apical localization and clustering.

Cytosolic Ca^{2+} Downstream of AKH Regulates GRASP Localization and Upd2 Secretion

Next, we asked whether there was a specific molecular connection between CaMKII and the nutrient-deprived state. Glucagon, the catabolic hormone that is the primary mediator of the starvation response, increases cytosolic Ca^{2+} levels by activating the inositol-3-phosphate receptor (IP3R) channel on the ER (Burgess et al., 1984). In some contexts CaMKII is activated by glucagon (Ozcan et al., 2012, 2013). Thus, we tested whether glucagon-like signaling in flies couples systemic energy status with Upd2 secretion.

In fat cells, AKH, the *Drosophila* functional analog of glucagon (Kim and Rulifson, 2004), signals through the AKH receptor (AKHR) (Gronke et al., 2007) to control lipolysis in response to starvation. Similar to prior work, we found that flies were unable to break down stored fat during starvation when *AKHR* was removed from fat cells (Figure S4A). We examined the presence of GRASP apical clustered localization during starvation in fat cells that lack *AKHR* (Figure 4A), and observed that GRASP continues to be present in apical sections even under starvation conditions (Figure 4Ad), whereas it is not present in controls (Figure 4Ab). Given that affecting the AKH response in fat cells is sufficient to retain GRASP apical localization in starved flies. This suggests that GRASP responds to systemic energy state downstream of gucagon-like signaling.

Next, we tested whether cytosolic Ca^{2+} influx due to glucagon-like signaling acts as a second messenger in terms of relaying AKH signal to GRASP. We assayed the effect of reducing the function of IP3R, the ER Ca^{2+} channel that responds to AKH, and observed that RNAi of *IP3R* in fat cells resulted in continued presence of GRASP clusters (Figure 4B). These results provide evidence for the role of cytosolic Ca^{2+}, downstream of glucagon-like signaling, in regulating GRASP localization during nutrient deprivation.

Previous studies have reported that flies mutant for *IP3R* are obese and do not break down lipid stores during starvation (Subramanian et al., 2013); however, it is unclear whether this is due to a fat cell-specific role of IP3R. We examined the effect of starvation on TAG levels in flies with fat cell-specific *IP3R* knockdown and observed that they were unable to break down fat stores (Figure 4C), resembling *upd2* overexpression in the fat body (Rajan and Perrimon, 2012). This suggests an antagonistic link between increased cytosolic Ca^{2+} levels and Upd2 action on fat storage. To test whether Upd2 and IP3R affects the same fat storage pathway, we compared the fold change in fat storage of *IP3R* knockdown in flies overproducing Upd2 versus a heterologous protein (GFP). While *IP3R* knockdown flies are obese (3.5- to 5-fold increase in fat stores) in comparison with control flies in a normal background (Figure 4Da), overproduction of *upd2* in *IP3R* knockdown flies did not significantly increase their fat stores (Figure 4Db), suggesting that Upd2 acts downstream of IP3R. To test the effect of cytosolic Ca^{2+} on Upd2 secretion, we used S2R+ cells as it is not technically feasible to assay Upd2 secretion in the adult fly hemolymph. Upd2 is secreted constitutively by S2R+ cells (Hombria et al., 2005; Wright et al., 2011), most likely because S2R+ cells lack the components to respond to glucagon/AKH signaling (fly glucagon AKH expression amount = 0.639, and the glucagon receptor AKHR = 0.000 based on RNA sequencing analysis data from modENCODE project [Hu et al., 2017]). But S2R+ cells express Ca^{2+} signaling components such as IP3R and CaMKII. Hence this cell system allows us to test specific predictions of our model downstream of glucagon. We altered cytosolic Ca^{2+} levels and activity by treating S2R+ cells with the Ca^{2+} chelator BAPTA-AM, phospholipase C (PLC) inhibitor that reduces IP3 levels (U73122), or the CaMKII inhibitor KN93, and observed enhanced Upd2 secretion (Figure 4E). Conversely, treatment with the Ca^{2+} ionophore ionomycin, which increases cytosolic Ca^{2+}, impaired Upd2 secretion (Figure 4E). Note that the data are represented as percent change in Upd2 secretion normalized to transfection efficiency (see STAR Methods) with 0% (DMSO) as baseline. We also tested whether the effects on Upd2 secretion were post-transcriptional. On performing real-time qPCR analysis of steady-state GRASP and Upd2 levels, we found that BAPTA-AM and KN93 did not affect *upd2* and *GRASP* transcription (Figure S4B). Further, the effect of the PLC inhibitor on transcription was not coupled to its effects on Upd2 secretion or GRASP regulation (Figure S4B). Finally, although the Ca^{2+} ionophore repressed *GRASP* transcription, it did not alter *upd2* transcription (Figure S4C). Our results on the post-transcriptional effect of cytosolic Ca^{2+} channel on Upd2 (Figure S4B) are consistent with a report that knockdown of the *Drosophila* store-operated Ca+ entry regulator *dStim* does not regulate *upd2* transcription (Baumbach et al., 2014). However, we did find that *dStim* knockdown increased Upd2 secretion (Figure S4D). We propose that increased Upd2 secretion in *dStim* knockdown explains in part the obese phenotype of *dStim* mutants (Baumbach et al., 2014). Altogether, we manipulated Ca^{2+} signaling in S2R+ cells, and show that increased Ca^{2+} signaling inhibits basal Upd2 secretion.

Upd2 is constitutively secreted, circulating at a "basal" level to indicate a "fed" state systemically. Our results point to a model in which, during nutrient deprivation, cells use cytosolic Ca^{2+} spikes downstream of glucagon as a negative signal for adipokine secretion.

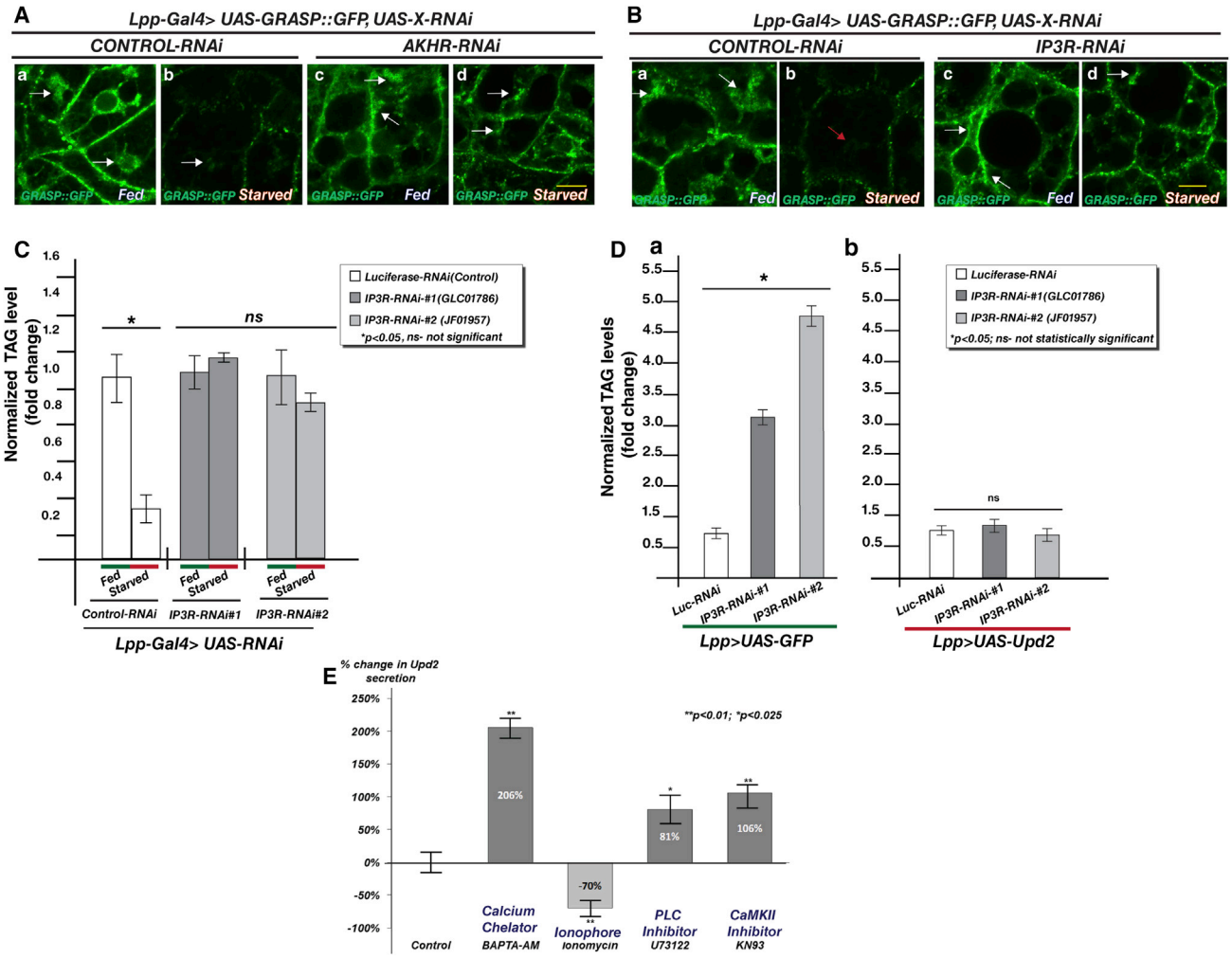

Figure 4. Intracellular Ca^{2+} Levels Affect GRASP Localization in Fat Cells and Upd2 Secretion

(A) Representative confocal images from adult fly fat cells expressing GFP-tagged GRASP with fat cell-specific reduction in the receptor for fly glucagon, adipokinetic hormone receptor (AKHR) (*AKHR-RNAi*), compared with control (*GFP-RNAi*). Compare the presence of clustered GRASP apical localization (arrow) in fed conditions (a and c) with starved conditions (b and d). Note the continued presence of apically localized GRASP in *AKHR* knockdown (d) in starved conditions compared with control (b). Note that images acquisition for all was performed with the same settings. See also Figure S4A which shows that flies with *AKHR* knockdown in fat cells are unable to break down triglyceride stores on starvation. Scale bar, 5 μm.

(B) Representative images from an apical section of adult fly fat cells expressing GFP-tagged GRASP with fat cell-specific reduction in the ER inositol-3-phosphate receptor (IP3R) (*IP3R-RNAi*) compared with control (*GFP-RNAi*). Compare the presence of GRASP apical structures (arrow) in fed (a and c) versus starved (b and d) conditions. Note the continued presence of GRASP apical localization in *IP3R* knockdown (d) in starved conditions compared with control (b). The effect of *IP3R* removal on GRASP hubs during starvation (Bd) is similar to *AKHR* knockdown (Ad). See also (C) showing that flies with *IP3R* knockdown in fat cells are unable to break down triglyceride stores under starvation conditions. Scale bar, 5 μm.

(C) Quantification of relative normalized TAG levels in starved flies compared with fed state, with fat cell-specific knockdown of two independent *IP3R* knockdown (*IP3R-RNAi*) and control (*GFP-RNAi*). Note that the starved control has significantly reduced fat content compared with *IP3R-RNAi* flies that exhibit defects in fat breakdown upon starvation.

(D) Effect of fat cell-specific Upd2 overexpression (*UAS-Upd2*) relative to GFP overexpression (*UAS-GFP*) in *IP3R* knockdown strains (*IP3R-RNAi*), compared with control (*Luciferase-RNAi*). Relative normalized TAG levels are quantified. Note that *IP3R* removal in fat cells causes a 3- to 5-fold increase in fat stores compared with control in GFP overexpression background. *IP3R* knockdown in an *Upd2* overexpression background does not significantly increase fat stores relative to control RNAi. Three biological replicates per data point, error bars represent %SD. Two-tailed t test was performed to determine statistical significance.

(E) Quantification of normalized fold change in secreted GFP signal detected by GFP sandwich ELISA assay performed on conditioned medium of S2R+ cells transfected with *Upd2::GFP* and treated with DMSO (control) or BAPTA-AM (5 μM), ionomycin (5 μM), U73122 (2 μM), and KN93(100 nM) for 18 hr. Error bars represent %SD. Statistical significance quantified by t test on six biological replicates per condition. $^{**}p < 0.01$, $^{*}p < 0.025$. Refer to companion Figure S4 for effect of Ca^{2+} drugs on *Upd2* and *GRASP* transcription.

See also Figure S4.

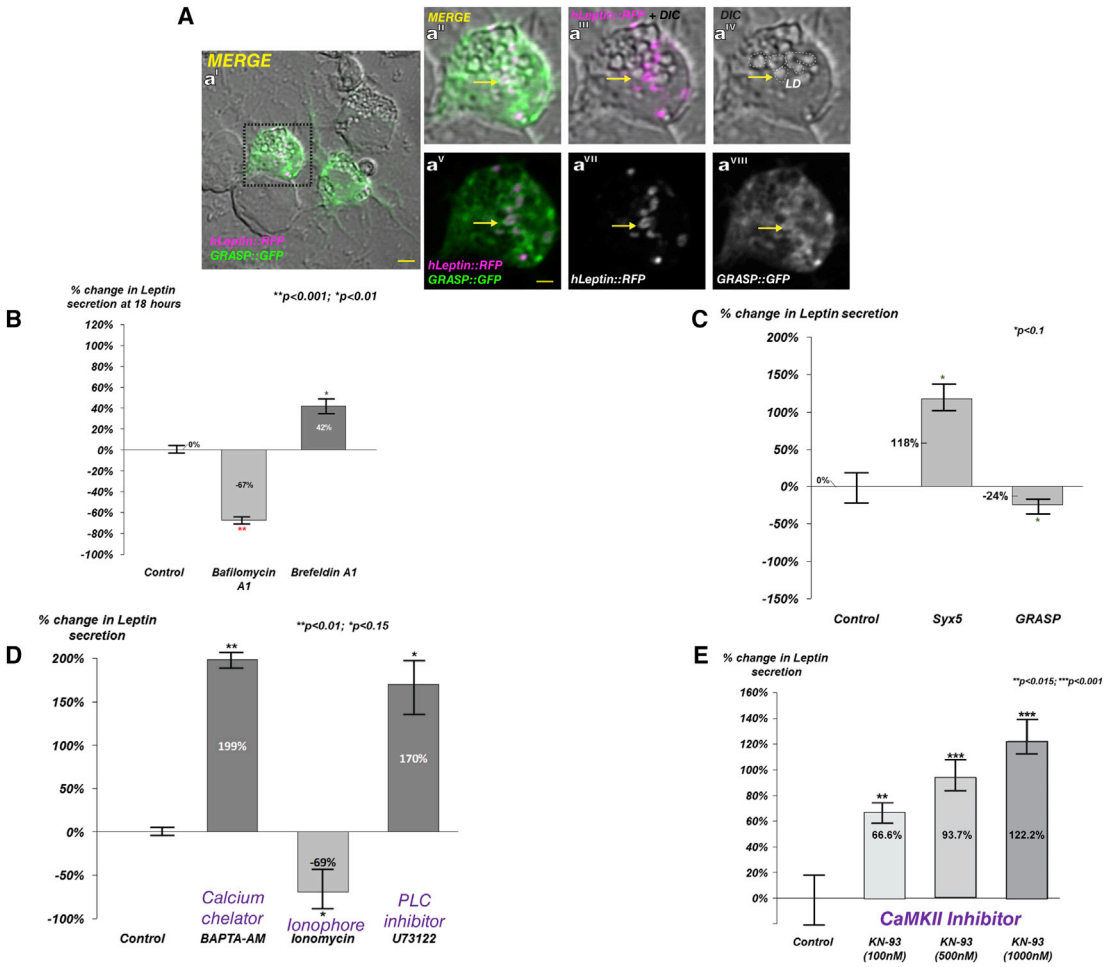

Figure 5. Human Leptin (hLeptin) Adopts an Unconventional Secretion Route in *Drosophila* Cells that Is Regulated by Intracellular Ca^{2+} via CaMKII

(A) S2R+ cells, loaded with oleic acid for 24 hr to accumulate LDs, were transiently transfected with GRASP::GFP (green) and human Leptin::RFP (hLeptin, magenta). Aa^{I}–Aa^{VII} are high-magnification confocal micrographs of Aa^{I}. hLeptin is observed at the LD periphery (a^{III}, a^{VI}, yellow arrow). GRASP-positive staining is observed at these locations (a^{II}, a^{V}, yellow arrow). Scale bars, 2 μm.

(B) Quantification of normalized fold change in secreted GFP signal detected using a GFP sandwich ELISA assay performed on conditioned medium of S2R+ cells transfected with *hLeptin::GFP*, and treated with DMSO (control) and the drugs Brefeldin A1 (5 μM) and Bafilomycin A1 (200 nM) for 18 hr. Error bars represent %SD. Statistical significance quantified by t test on six biological replicates per condition.

(C) Relative normalized secreted GFP signal detected by GFP sandwich ELISA assay performed on conditioned medium of S2R+ cells incubated with dsRNAs targeting *LacZ* (control), *Drosophila syntaxin* 5 (*Syx5*), or *GRASP*. Statistical significance quantified by t test on six biological replicates per condition.

(D) Quantification of relative normalized secreted GFP signal detected by GFP sandwich ELISA assay performed on conditioned medium of S2R+ cells transfected with *hLeptin::GFP* and treated with DMSO (control) and the drugs BAPTA-AM (5 μM), ionomycin (5 μM), and U73122 (2 μM). Error bars represent %SD. Statistical significance quantified by t test on six biological replicates per condition.

(E) Dose-sensitive increase in hLeptin::GFP secretion following CaMKII inhibition in S2R+ cells. Quantification of relative normalized secreted GFP signal detected by GFP sandwich ELISA assay performed on conditioned medium of S2R+ cells transfected with *hLeptin::GFP* and treated with indicated amounts of CaMKII inhibitor KN93. Error bars represent %SD. Statistical significance quantified by t test on six biological replicates per condition.

Human Leptin Localizes with GRASP in *Drosophila* Cells, and Its Secretion Is Regulated via the Cytosolic Ca^{2+} Sensing Kinase CaMKII

Previously, we showed that Upd2 is an ancestral functional ortholog of human leptin (hLeptin), specifically in the context of remotely conveying systemic nutrient status (Rajan and Perrimon, 2012). Thus, we examined the cytoplasmic localization of hLeptin in *Drosophila* cells and asked if its localization and secretion also requires GRASP.

In lipid-loaded S2R+ cells cultured with oleic acid, hLeptin localized to LD periphery and appeared to co-localize with GRASP (Figure 5A). In addition, adding Bafilomycin A1 in S2R+ cells severely impaired hLeptin secretion, whereas BFA had no effect (Figure 5B), consistent with our observations for Upd2 secretion (Figure 1A). Further, impairment of conventional secretion by knockdown of *Syntaxin5 (Syx5)* did not reduce hLeptin secretion, and in fact led to upregulation (Figure 5C), whereas knocking down *GRASP* caused a modest but significant

reduction of hLeptin secretion (Figure 5C), indicating that the unconventional secretion machinery is required for hLeptin secretion.

Finally, we tested the effect of cytosolic Ca^{2+} on hLeptin secretion by manipulating Ca^{2+} levels in S2R+ cells expressing hLeptin. Similar to the results with Upd2 (Figure 4E), hLeptin secretion was upregulated by the cytosolic Ca^{2+} chelator BAPTA-AM, but was inhibited by the Ca^{2+} ionophore ionomycin, and was upregulated by IP3R inhibition (Figure 5D). In agreement with our results on the role of CaMKII in Upd2 secretion, hLeptin secretion displayed a dose-dependent increase during CaMKII inhibition (Figure 5E). Altogether these results show that hLeptin secretion in a heterologous system behaves as Upd2 and is negatively regulated by cytosolic Ca^{2+} levels and CaMKII.

In Adult *Drosophila* Fat Cells GRASP and Upd2 Are Apically Enriched in Close Apposition to LDs

Given that GRASP is required for Upd2 secretion (Figures 1B and 2D) and for Upd2 to exert its physiological effects on fat storage (Figure 2E), we were interested in visualizing GRASP and Upd2 cellular localization in fat cells (see STAR Methods and Figure S5A). In the subsequent descriptions the term "Apical" refers to the surface of the fat cell that is in contact with the lumen and hemolymph, and "Basal" is the side of the fat cell that is attached to the cuticle (refer to diagrams in Figures 6 and S5A for orientation).

GFP-tagged GRASP (*UAS-GRASP::GFP*), which is functional and able to rescue *GRASP-del* mutants (Figure 2C), was expressed in fly fat cells using the fat body-specific driver Lpp-Gal4 and co-stained with antibodies to the LD-associated protein PERILIPIN1 (PLIN1) (Beller et al., 2010) (Figure 6A). Confocal imaging analyses revealed that GRASP exhibits a widely distributed cytoplasmic and membrane localization (Figures 6Aa and S5B). GRASP localization can be broadly characterized to distinct locations (Figures 6Ab and S5B) that include: (1) the ring periphery of LDs (Figures 6Ab and S5Ba); (2) the clustered GRASP enrichment periphery of the LDs (Figures 6Ab, 6Ac, and S5Bb); and (3) the cytosolic punctae and plasma membrane (Figure S5Bc). Specifically, on examining the most apical sections (at 2–4 μM from the apical surface of the cell), we observed GRASP enrichment juxtaposed to the LD surface (see pink arrows, Figures 6Ab and 6Ac). While PLIN1 exhibited approximately equal apico-basal distribution (Figure 6Ac), GRASP localization was skewed to the apical side of the cell (Figure 6Ac).

The localization of GRASP at close apposition to the LD periphery is not due to its myristoylation motif as GRASP in fat cells expressing myristoylated GFP (myr::GFP) under the same conditions as GRASP::GFP does not localize to LD proximity (Figure S5C).

Given the role of GRASP in Golgi organization (Barr et al., 1997a), we examined Golgi markers in conjunction with GRASP (Figure S5D). We observed that the punctate vesicles localized with Golgi, but "circular" GRASP localization in the apical periphery of the LDs did not (Figure S5D), suggesting that GRASP localization in the LD periphery is not associated with its Golgi localization (see Discussion).

Upd2 distribution in adult fat cells was assayed by expressing a tagged version of Upd2 (*Lpp-Gal4> UAS-Upd2::TagRFP-T*). We detected a cytoplasmic vesicular distribution of Upd2, with an enrichment at the LD periphery (Figure 6Ba′). Also, the Upd2 signal was enriched in planes apical to the nucleus (approximately 4 μM from cell surface, compare Figures 6Ba′ and 6Ba‴; see orthogonal view Figure 6Bb). Next, we examined the localization of Upd2 with respect to GRASP in fat cells of transgenic flies expressing differentially tagged forms of GRASP and Upd2 (*Lpp-Gal4> UAS-Upd2::TagRFP-T, UAS-GRASP::GFP*). Upd2 localized close to the GRASP compartments at the periphery of LDs (Figure 6Ca) at the apical side of fat cells (4 μM from cell surface). Further, orthogonal sections through fat cells along the xz axis revealed that the co-localization between GRASP and Upd2 increases in sections apical to the nuclear plane (Figure 6Cb).

Overall, we observe that both Upd2 and GRASP display an apico-basal polarity in their distribution in fat cells and in more apical regions of the cell localize in close proximity to LDs.

GRASP Localization in *Drosophila* Adult Fat Cells Is Dependent on Systemic Nutritional Status and Regulated by Cytosolic Calcium

Next, we asked whether the apical-basal polarity of GRASP (Figure 6Ac) and GRASP clustering was influenced by altered nutritional status. Adult males expressing GRASP::GFP in their fat cells were subjected to a starvation regime. We imaged optical sections through fat tissue from fed and starved flies under the same imaging conditions and analyzed GRASP distribution in fat cells in all optical planes (Figures 7a′ and 7b′). We observed a reduction in the intensity of GRASP apical localization in the starved state (Figure 7B, compare sections 4–10 in fed [Figure 7a′] versus starved [Figure 7b′] fat tissue). Significantly, at more basal compartments, GRASP punctae were higher in starved versus fed fat tissue (Figure 7B, compare sections 11–20 in fed [Figure 7a′] versus starved [Figure 7b′] fat tissue). The same effect of systemic nutrient state on GRASP apical localization was observed when GRASP was tagged with a different fluorophore (Figure S6A), suggesting that this is not due to a particular protein tag. The reduction in GRASP levels is likely an effect of reduced protein synthesis during starvation, which is consistent with what we observe by western blot analysis (Figures 3A, 3B, S3A, and S3D). Nevertheless, we note that GRASP was preferentially basally localized in starved fat cells (see Figure 7Ab′, sections 11–20), whereas it displays a marked apical localization in the well-fed state.

As described previously, in standard lab food conditions, GRASP is distributed at the membrane, LD periphery, and cytosolic punctae (Figure S5B). We sought to identify whether any particular pool of cytoplasmic GRASP was most sensitive to starvation or whether all pools were equally affected by reduction in protein levels. We performed image segmentation analysis on z stacks from fed and starved cells (see Figure S6B and the STAR Methods) and queried the percentage of area occupied by each pool in the entire fat cell. Our analysis revealed that clustered GRASP (5% in fed versus 0.1% in starved) and membrane localized GRASP (14% in fed versus 1.1% in starved) were significantly reduced during starvation (>92% reduction) compared with well-fed states (see graph in Figures 7Aa″ and 7Ab″). However, the punctate GRASP localization is largely insensitive to low-energy states, (approximately 40% of GRASP

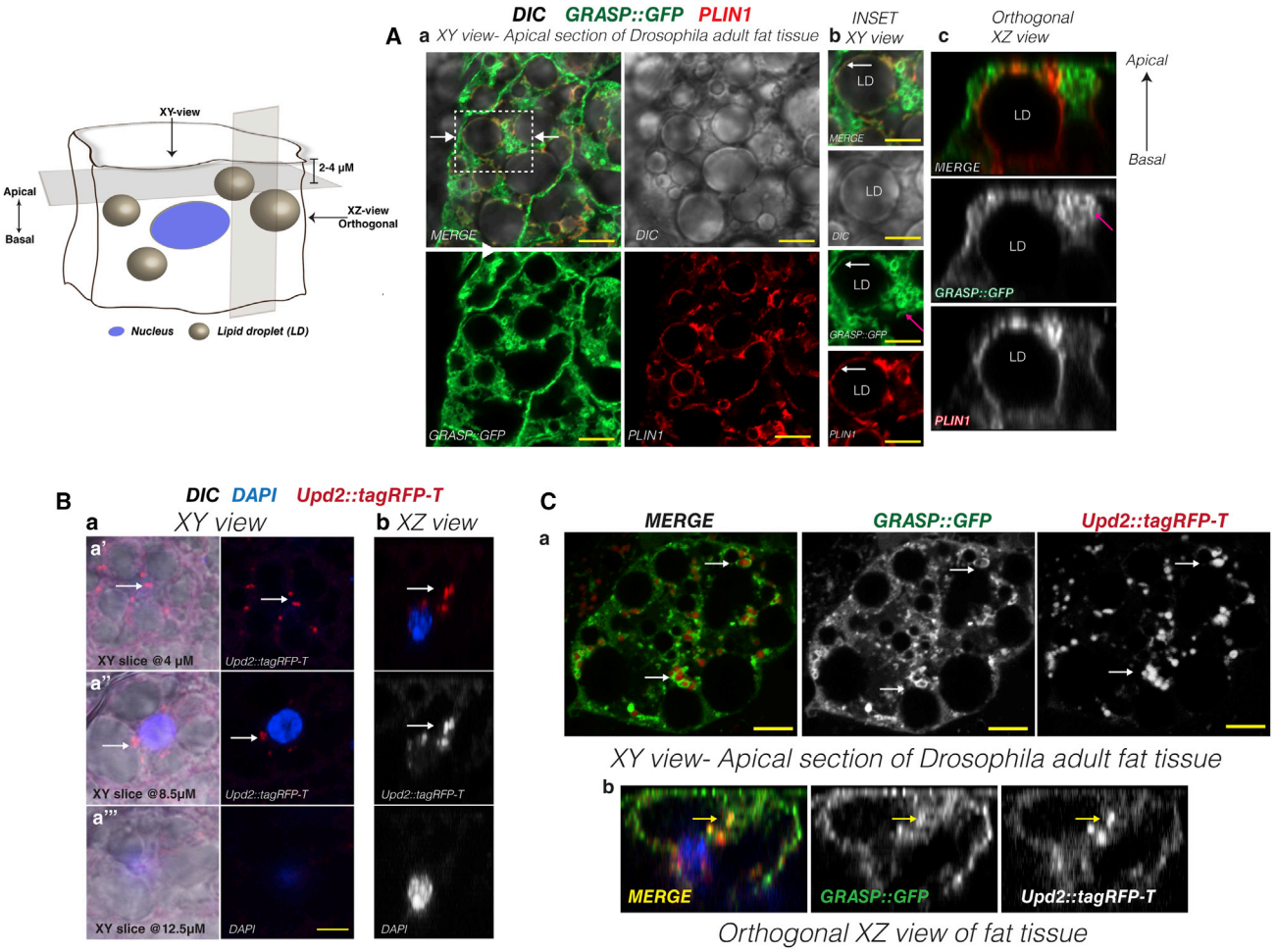

Figure 6. Distribution of Tagged GRASP and Upd2 in Adult *Drosophila* Fat Cells

The diagram depicts the orientation (xy and xz) and depth of apical sections (2–4 μM) during laser scanning confocal acquisition. Note "Apical" refers to the surface of the fat cell that is in contact with the lumen and hemolymph, and "Basal" is the side of the fat cell that is attached to the cuticle. See diagram in companion Figure S5A for adult *Drosophila* fat tissue preparation used for imaging.

(A) Single optical section of *Drosophila* adult fat tissue expressed GFP-tagged GRASP (green) stained with anti-perilipin1 (PLIN1) antibody (red). PLIN1 is used as a marker for LD surface. (a) Confocal image of a single optical section along the xy axis at the apical side of adult *Drosophila* fat cells expressing GFP-tagged GRASP. Note the wide cytoplasmic distribution of GRASP (see Figure S5B). Box is location of inset shown in (b) and arrows point to location where the xz slice (c) was acquired. GRASP exhibits a wide cytoplasmic distribution, but exhibits specificity in its localization to LD periphery. Note that control myristoylated GFP proteins do not exhibit this localization (Figure S5C), and that GRASP also forms "clusters" in the most apical sections. (b) High-magnification view to show clusters (pink arrow) and LD peripheral localization (white arrow) of GRASP. (c) Orthogonal yz axis view of GRASP localization. Note the concentration of GRASP "clusters" on the apical side of the cell (pink arrows), while PLIN1 displays approximately equal distribution from basal to apical.

(B) (a) Confocal micrograph representing an xy view of fat cells expressing Upd2::tagRFP-T (red) and nucleus (blue); differential interference contrast reveals LD. White arrows point to Upd2 punctae; xy serial sections from apical (a′) at 4 μM depth from the top of the cell to basal (a‴) at a depth of 12.5 μM. (b) yz slice orthogonal view. Note that the Upd2 punctae are enriched at a plane above the nucleus.

(C) Confocal micrographs of optical sections of adult fat tissues expressing tagged Upd2 and GRASP (Upd2::tagRFP-T in red, GRASP::GFP in green, and nucleus in blue). (a) xy view of fat cell at 4 μM depth. Upd2 punctae appear in the proximity of GRASP enriched regions. (b) Orthogonal view along the xz axis. Arrow points to the co-localization of GRASP and Upd2 in a sub-apical location above the plane of the nucleus.

Scale bars, 5 μm (in micrographs Figures 6A–6C). See also Figure S5.

was detected as punctae in both states). The observation, that specific GRASP pools, especially those that are likely formed by oligomerization, are most sensitive to starvation, correlates with increased GRASP phosphorylation (Figures 3A, 3B, and S3A), and consistent with prior reports that GRASP phosphorylation results in GRASP "unlinking" (Wang et al., 2005; Yoshimura et al., 2005).

The role of cytosolic Ca^{2+}, downstream of glucagon-like signaling, in regulating GRASP localization during nutrient deprivation (Figures 4A and 4B), prompted us to ask whether specific pools of GRASP were sensitive to Ca^{2+} during nutrient deprivation. Therefore we assayed GRASP localization during starvation while manipulating cytosolic Ca^{2+} levels. We starved flies in the presence of PLC inhibitor, U73122, which causes defects in

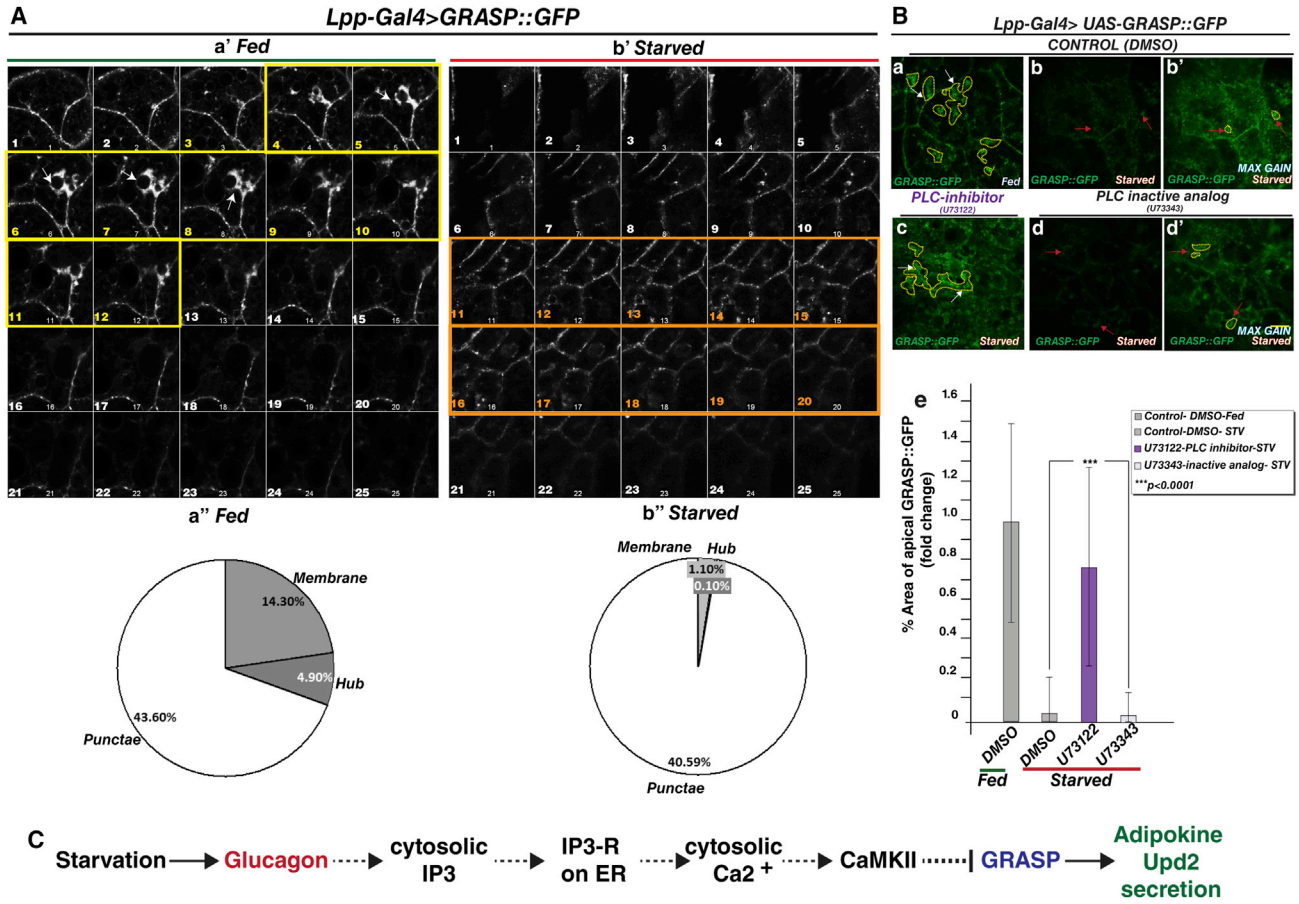

Figure 7. GRASP Localization in *Drosophila* Adult Fat Cells Is Dependent on Systemic Nutritional Status and Regulated by Cytosolic Calcium

(A) Confocal images documenting the expression of GRASP::GFP in adult fat tissue under normal food (a′) and starvation (b′). Montage of the xy stack from apical to more basal sections (optical slices 1–25). In the fed state (a′) note the presence of high-intensity GRASP localization in apical sections (arrow in slice 8, yellow framed slices) compared with similar sections in the starved state. In contrast, a higher intensity of GRASP punctae are observed in mid-basal slices (orange framed slices) in starved (b′) and reduced basal localization of GRASP in fed state (a′) in optical slices 14–20. Note images acquired under same settings for both conditions. GRASP tagged with another fluorophore shows a similar change in localization in the starved state (see companion Figure S6A). (a″ and b″) Quantification of %area of GRASP GFP pixels localization to specific compartment. These are subdivided into three categories (punctae, membrane, and hubs). Note that while the membrane and "hub" localization of GRASP is significantly reduced in the starved state, the punctate localization (~40%) remains similar. See Figure S6B for details on image segmentation and on how %area was computed.

(B) To test the effect of acutely inhibiting cytosolic Ca^{2+} efflux downstream of glucagon-like signaling on GRASP hubs during starvation, flies expressing GFP-tagged GRASP (a) were starved in the presence of vehicle DMSO (b), PLC inhibitor (U73122, see c), or an inactive analog of PLC inhibitor (d). Confocal images were captured at an apical plane from *Drosophila* fat explants. Note the continued presence of GRASP localization in "clusters" when PLC is inhibited (c, outlined in yellow) in starved conditions compared with controls (b and d). The %area of GRASP localization in the apical clusters (outlined in yellow dashed lines) is quantified relative to the fed control (e). The persistent GRASP localization compared with control drugs is statistically significant and comparable with the fed state. Image acquisition was performed with the same settings and five to seven fat explants from different animals were used for quantification per data point. Note b′ and d′ show higher gain images of b and d to allow visualization of GRASP::GFP. See companion Figure S6B for details on quantification. Two-tailed t test was performed to calculate statistical significance. Error bars represent %SD.

(C) Working model derived from the results.

Scale bars, 5 μm (in all micrographs). See also Figure S6.

cytosolic IP3R production (Bleasdale et al., 1990) and hence will affect the release of Ca^{2+} from the ER. We observed that treatment of flies with PLC inhibitor causes persistent apical GRASP clusters during starvation (Figure 7Bc) compared with controls (Figure 7Bb and 7Bd); this effect is statistically significant (Figure 7Be; quantified using image segmentation analysis Figure S6B). These results suggest that the apical localization of GRASP to LD proximity is most sensitive to nutrient levels and is regulated by cytosolic Ca^{2+} increases downstream of IP3R.

DISCUSSION

How adipokines are released from adipocytes depending on energy store levels is an outstanding question in physiology. Previously, we documented that Upd2 is produced from fat cells in response to dietary fat and sugars (Rajan and Perrimon, 2012). In the present study, we describe how Upd2 secretion depends on GRASP, a component of the unconventional secretion pathway. We demonstrate a surprising antagonistic effect of

increased cytosolic Ca^{2+} on adipokine secretion. We show that this negative regulation is at least in part the effect of CaMKII-mediated phosphorylation of the unconventional secretion component GRASP.

A Novel Role for GRASP

GRASP, a myristoylated PDZ-domain, has two mammalian isoforms, GRASP55 and GRASP65, but only one isoform, in flies. It has been previously implicated in a number of processes including Golgi stacking (Barr et al., 1997a) and, unconventional secretion from amoeba (Kinseth et al., 2007), to humans (Gee et al., 2011). Here, we found that *GRASP* mutants have lipid storage defects that phenocopy *upd2* mutants (Figure 2A) and that the role of GRASP in fat storage is tissue specific (Figure 2B). Future work will resolve how GRASP-mediated trafficking causes the adipokine to be released from the cell.

Whether our findings regarding GRASP's role in adipokine secretion are relevant to higher-order model systems requires studies in mammalian models. GRASP65 mutant mice appear viable and fertile, but detailed information on its energy physiology is lacking (Veenendaal et al., 2014). Furthermore, experiments have suggested that GRASP65 and GRASP55 play redundant roles (Xiang and Wang, 2010), hence examination of double-mutant mice will likely be important to characterize the role of GRASP in energy physiology.

We have shown, using different assays, that Upd2 adopts an unconventional secretion route (Figures 1 and S1). However, we note that it is unexpected that Upd2 is glycosylated (Figure S1) even though there is no "traditional" ER-targeting signal in the Upd2 protein sequence. Further studies will be required to clarify the mechanisms governing Upd2 glycosylation in the absence of an ER-targeting signal. One possibility is that Upd2 has a "hidden" signal sequence that needs further characterization. Since we observe that Upd2 localizes in close apposition to LDs (see Figure 6C), another probable mechanism could be glycosylation by LD localized glycosyltransferases (Krahmer et al., 2013).

GRASP Apical Localization

GRASP hubs are positioned at LD proximity, and others have reported that ER-Golgi intermediate compartments (ERGIC) are found at close juxtaposition to the LD, and demonstrated that trafficking of LD-associated proteins occurs via this compartment (Soni et al., 2009). Our observations with GFP-tagged GRASP are reminiscent of these findings and other studies that have shown that GRASP is present at both the Golgi and the ERGIC (Marra et al., 2001). Whether and how these GRASP clusters interact with ERGIC will require future studies, and we were unable to resolve those using antibodies to ERGIC components and conventional fluorescence microscopy (data not shown). Super-resolution microscopy on tagged components of ERGIC and GRASP should clarify whether ERGIC/ERES localize with GRASP "clusters."

A caveat of our work is that we have used tagged versions of Upd2 and GRASP in these studies because of limitations related to a lack of antibodies that recognize endogenous protein in fat tissue by immunohistochemistry. Nevertheless, the tagged versions we used have been tested for functionality and hence are a useful surrogate for endogenous localization.

Disruption of Ca^{2+} Homeostasis and Obesity

Previous studies in both mammals and flies have suggested that dysfunctional Ca^{2+} homeostasis is linked to obesity, although the mechanism underlying this phenomenon is unclear. In mammals under starvation, glucagon triggers an IP3R-mediated transcriptional program in hepatocytes to promote survival during fasting (Wang et al., 2012). In addition, studies of glucagon action in mice have shown that CaMKII is activated by glucagon in hepatocytes to regulate insulin sensitivity (Ozcan et al., 2012, 2013), and that dysregulation of Ca^{2+} homeostasis leads to obesity (Fu et al., 2011). In flies, a number of studies have reported that mutations in genes that alter cytosolic Ca^{2+} levels cause changes in fat storage (Baumbach et al., 2014; Bi et al., 2014; Moraru et al., 2017; Subramanian et al., 2013). Nevertheless, the mechanistic basis for how Ca^{2+} levels and fat storage are linked has remained unclear. Our study, showing that increased cytosolic Ca^{2+}, by negatively regulating GRASP via CaMKII-mediated phosphorylation, affects Upd2 secretion, provides a specific molecular pathway linking Ca^{2+} to fat storage. Importantly, the pathway we have identified is likely evolutionarily conserved as we find that hLeptin secretion adopts an unconventional secretion route, and, like Upd2, is negatively regulated by increased cytosolic Ca^{2+} and CaMKII activity.

Implications of Upd2 Secretion for Understanding Leptin Release

As leptin rescues *upd2* mutants and is structurally similar to Upd2, it is likely that the mechanism we identified for Upd2 secretion is relevant to leptin production. However, unlike Upd2, leptin possesses a signal peptide, and has been reported to localize to the ER (Barr et al., 1997b; Roh et al., 2000). Leptin has two strongly predicted disulfide bonds (two bonds predicted with score of 0.98; score of 1 being 100% probability). In contrast, Upd2 has no high-scoring disulfide bonds (three predicted bonds with highest score of 0.014); predictions were made using DiANNA, an artificial neural network web tool for ternary cysteine classification and disulfide bond prediction (Ferre and Clote, 2006). Since disulfide-bridge-forming enzymes are ER localized (Frand and Kaiser, 1998), the signal sequence of leptin and its ER localization is probably a requirement for its proper folding.

A number of proteins with conventional secretion signals, such as *Drosophila* α-integrin, human CFTR, and CD45, are ER-targeted proteins, which bypass the Golgi (Grieve and Rabouille, 2011). Thus, it is possible that leptin, similar to Upd2, does not traffic through the Golgi. In support of the Golgi bypass model for leptin, two studies carried out in rat primary adipocytes and adipose tissue explants (Barr et al., 1997b; Roh et al., 2000), using immunofluorescence and sucrose gradient centrifugation, did not find evidence for leptin Golgi localization. These studies favored a model that leptin is released via "special" secretory vesicles that are devoid of other adipocyte secretory products (Barr et al., 1997b; Lee and Fried, 2006; Roh et al., 2000). Whether these vesicles correspond to GRASP-positive compartments will need to be investigated. Leptin and Upd2 likely arose from the need to remotely signal systemic nutrient status (Ahima et al., 1996; Flier and Maratos-Flier, 2017; Rajan and Perrimon, 2012). Hence our findings on how Upd2 secretion from fly

fat cells is coupled to energy levels is likely to be relevant to mammalian adipokine production.

STAR★METHODS

Detailed methods are provided in the online version of this paper and include the following:

- KEY RESOURCES TABLE
- CONTACT FOR REAGENT AND RESOURCE SHARING
- EXPERIMENTAL MODEL AND SUBJECT DETAILS
  - Experimental Animals
  - Cell Lines
- METHOD DETAILS
  - Tissue Culture
  - dsRNA Production and Cell Treatments
  - Treatment of Cells with Drugs
  - ELISA Assays
  - Renilla Luciferase Assay
  - Endo H Sensitivity Assay
  - Cloning
  - Immunoprecipitation, Mass Spectrometry, and Western Blots
  - Recombinant Protein Expression
  - *In vitro* Kinase Assay and Phosphoprotein Blot Stains
  - TAG Assay
  - Generation of GRASP CRISPR Mutant
  - Nutrient Deprivation and Drug Feeding
  - Adult Brain Immunostaining
  - Fat Body Preparation for Fixed Immunostaining and *Ex Vivo* Assays
- QUANTIFICATION AND STATISTICAL ANALYSIS
  - Image Analysis Quantification
  - ELISA
  - TAG Assays

SUPPLEMENTAL INFORMATION

Supplemental Information includes six figures and can be found with this article online at https://doi.org/10.1016/j.devcel.2017.09.007.

AUTHOR CONTRIBUTIONS

Conceptualization, Funding Acquisition, and Project Administration, A.R. and N.P.; Methodology, Data Curation, and Visualization, A.R.; Resources, B.H. and F.W.P.; Investigation, A.R. and L.H.; Writing – Original Draft, A.R.; Writing-Review & Editing, N.P.

ACKNOWLEDGMENTS

We thank R.P. Kühnlein for the generous gift of the PERILIPIN1 antibody, P. Leopold for sharing the Dilp5 antibody, and J.A. Lepesant for the gift of the Lsp1-gamma antibody; M. Freeman for Spitz::GFP construct; M. Zeidler, M. Freeman, S. Eaton, C.S. Goodman, P. Shen, the Transgenic RNAi facility (TRiP), and the Bloomington Drosophila Stock Center for flies; the Drosophila RNAi screening center (DRSC) for dsRNA reagents and plate reader equipment; Y. Hu at the DRSC for designing new GRASP amplicons; L. Perkins and A. Miller at the TRiP for generating GRASP-RNAi lines; and C. Villalta, S. Vora, M. Pyle, and M. Foos for technical assistance. Label-free quantitative MS for GRASP complex identification was performed at the BIDMC Mass Spectrometry core with the help of J. Asara. H. Elliot at the Image and Data analysis core (IDAC) at Harvard Medical School provided advice on segmentation methods and WEKA tool usage. We thank the Drosophila Genomics Resource Center (DGRC), supported by NIH grant 2P40OD010949, for GRASP cDNA clones. We are grateful to P. Jouandin and P. Raghavan for discussions and critical feedback. We thank S. Mohr, A. Petsakou, P. Saavedra, C. Xu, and A. Brent for critical comments on the manuscript. N.P is an investigator of the Howard Hughes Medical Institute. This project was supported by the NIH via grants P01CA120964 (awarded to N.P. by the National Cancer Institute) and K99/R00DK101605 (awarded to A.R. by the National Institute of Diabetes and Digestive and Kidney Diseases).

Received: January 9, 2017
Revised: July 18, 2017
Accepted: September 11, 2017
Published: October 9, 2017

REFERENCES

Ahima, R.S., Prabakaran, D., Mantzoros, C., Qu, D., Lowell, B., Maratos-Flier, E., and Flier, J.S. (1996). Role of leptin in the neuroendocrine response to fasting. Nature *382*, 250–252.

Baeg, G.H., Zhou, R., and Perrimon, N. (2005). Genome-wide RNAi analysis of JAK/STAT signaling components in *Drosophila*. Genes Dev. *19*, 1861–1870.

Bard, F., Casano, L., Mallabiabarrena, A., Wallace, E., Saito, K., Kitayama, H., Guizzunti, G., Hu, Y., Wendler, F., Dasgupta, R., et al. (2006). Functional genomics reveals genes involved in protein secretion and Golgi organization. Nature *439*, 604–607.

Barr, F.A., Puype, M., Vandekerckhove, J., and Warren, G. (1997a). GRASP65, a protein involved in the stacking of Golgi cisternae. Cell *91*, 253–262.

Barr, V.A., Malide, D., Zarnowski, M.J., Taylor, S.I., and Cushman, S.W. (1997b). Insulin stimulates both leptin secretion and production by rat white adipose tissue. Endocrinology *138*, 4463–4472.

Baumbach, J., Hummel, P., Bickmeyer, I., Kowalczyk, K.M., Frank, M., Knorr, K., Hildebrandt, A., Riedel, D., Jackle, H., and Kuhnlein, R.P. (2014). A *Drosophila* in vivo screen identifies store-operated calcium entry as a key regulator of adiposity. Cell Metab. *19*, 331–343.

Beller, M., Bulankina, A.V., Hsiao, H.H., Urlaub, H., Jackle, H., and Kuhnlein, R.P. (2010). PERILIPIN-dependent control of lipid droplet structure and fat storage in *Drosophila*. Cell Metab. *12*, 521–532.

Beshel, J., Dubnau, J., and Zhong, Y. (2017). A leptin analog locally produced in the brain acts via a conserved neural circuit to modulate obesity-linked behaviors in *Drosophila*. Cell Metab. *25*, 208–217.

Bi, J., Wang, W., Liu, Z., Huang, X., Jiang, Q., Liu, G., Wang, Y., and Huang, X. (2014). Seipin promotes adipose tissue fat storage through the ER Ca(2)(+)-ATPase SERCA. Cell Metab. *19*, 861–871.

Bleasdale, J.E., Thakur, N.R., Gremban, R.S., Bundy, G.L., Fitzpatrick, F.A., Smith, R.J., and Bunting, S. (1990). Selective inhibition of receptor-coupled phospholipase C-dependent processes in human platelets and polymorphonuclear neutrophils. J. Pharmacol. Exp. Ther. *255*, 756–768.

Brankatschk, M., and Eaton, S. (2010). Lipoprotein particles cross the blood-brain barrier in *Drosophila*. J. Neurosci. *30*, 10441–10447.

Burgess, G.M., Godfrey, P.P., McKinney, J.S., Berridge, M.J., Irvine, R.F., and Putney, J.W., Jr. (1984). The second messenger linking receptor activation to internal Ca release in liver. Nature *309*, 63–66.

Burmester, T., Antoniewski, C., and Lepesant, J.A. (1999). Ecdysone-regulation of synthesis and processing of fat body protein 1, the larval serum protein receptor of *Drosophila* melanogaster. Eur. J. Biochem. *262*, 49–55.

Chen, Y., Wei, L.N., and Muller, J.D. (2003). Probing protein oligomerization in living cells with fluorescence fluctuation spectroscopy. Proc. Natl. Acad. Sci. USA *100*, 15492–15497.

Dascher, C., Matteson, J., and Balch, W.E. (1994). Syntaxin 5 regulates endoplasmic reticulum to Golgi transport. J. Biol. Chem. *269*, 29363–29366.

Dugail, I., and Hajduch, E. (2007). A new look at adipocyte lipid droplets: towards a role in the sensing of triacylglycerol stores? Cell. Mol. Life Sci. *64*, 2452–2458.

Duncan, R.E., Ahmadian, M., Jaworski, K., Sarkadi-Nagy, E., and Sul, H.S. (2007). Regulation of lipolysis in adipocytes. Annu. Rev. Nutr. *27*, 79–101.

Dupont, N., Jiang, S., Pilli, M., Ornatowski, W., Bhattacharya, D., and Deretic, V. (2011). Autophagy-based unconventional secretory pathway for extracellular delivery of IL-1beta. EMBO J. *30*, 4701–4711.

Farooqi, I.S., and O'Rahilly, S. (2009). Leptin: a pivotal regulator of human energy homeostasis. Am. J. Clin. Nutr. *89*, 980S–984S.

Ferre, F., and Clote, P. (2006). DiANNA 1.1: an extension of the DiANNA web server for ternary cysteine classification. Nucleic Acids Res. *34*, W182–W185.

Flak, J.N., and Myers, M.G., Jr. (2015). CNS mechanisms of leptin action. Mol. Endocrinol. *30*, 3–12, me20151232.

Flier, J.S., and Maratos-Flier, E. (2017). Leptin's physiologic role: does the emperor of energy balance have no clothes? Cell Metab. *26*, 24–26.

Frand, A.R., and Kaiser, C.A. (1998). The ERO1 gene of yeast is required for oxidation of protein dithiols in the endoplasmic reticulum. Mol. Cell *1*, 161–170.

Fried, S.K., Ricci, M.R., Russell, C.D., and Laferrere, B. (2000). Regulation of leptin production in humans. J. Nutr. *130*, 3127S–3131S.

Friggi-Grelin, F., Rabouille, C., and Therond, P. (2006). The *cis*-Golgi *Drosophila* GMAP has a role in anterograde transport and Golgi organization in vivo, similar to its mammalian ortholog in tissue culture cells. Eur. J. Cell Biol. *85*, 1155–1166.

Fu, S., Yang, L., Li, P., Hofmann, O., Dicker, L., Hide, W., Lin, X., Watkins, S.M., Ivanov, A.R., and Hotamisligil, G.S. (2011). Aberrant lipid metabolism disrupts calcium homeostasis causing liver endoplasmic reticulum stress in obesity. Nature *473*, 528–531.

Gee, H.Y., Noh, S.H., Tang, B.L., Kim, K.H., and Lee, M.G. (2011). Rescue of DeltaF508-CFTR trafficking via a GRASP-dependent unconventional secretion pathway. Cell *146*, 746–760.

Geminard, C., Rulifson, E.J., and Leopold, P. (2009). Remote control of insulin secretion by fat cells in *Drosophila*. Cell Metab. *10*, 199–207.

Grieve, A.G., and Rabouille, C. (2011). Golgi bypass: skirting around the heart of classical secretion. Cold Spring Harb. Perspect. Biol. *3*, http://dx.doi.org/10.1101/cshperspect.a005298.

Gronke, S., Muller, G., Hirsch, J., Fellert, S., Andreou, A., Haase, T., Jackle, H., and Kuhnlein, R.P. (2007). Dual lipolytic control of body fat storage and mobilization in *Drosophila*. PLoS Biol. *5*, e137.

Guo, Y., Walther, T.C., Rao, M., Stuurman, N., Goshima, G., Terayama, K., Wong, J.S., Vale, R.D., Walter, P., and Farese, R.V. (2008). Functional genomic screen reveals genes involved in lipid-droplet formation and utilization. Nature *453*, 657–661.

Hombria, J.C., Brown, S., Hader, S., and Zeidler, M.P. (2005). Characterisation of Upd2, a *Drosophila* JAK/STAT pathway ligand. Dev. Biol. *288*, 420–433.

Housden, B.E., Valvezan, A.J., Kelley, C., Sopko, R., Hu, Y., Roesel, C., Lin, S., Buckner, M., Tao, R., Yilmazel, B., et al. (2015). Identification of potential drug targets for tuberous sclerosis complex by synthetic screens combining CRISPR-based knockouts with RNAi. Sci. Signal. *8*, rs9.

Hu, Y., Comjean, A., Perrimon, N., and Mohr, S.E. (2017). The *Drosophila* gene expression tool (DGET) for expression analyses. BMC Bioinformatics *18*, 98.

Kim, S.K., and Rulifson, E.J. (2004). Conserved mechanisms of glucose sensing and regulation by *Drosophila* corpora cardiaca cells. Nature *431*, 316–320.

Kinseth, M.A., Anjard, C., Fuller, D., Guizzunti, G., Loomis, W.F., and Malhotra, V. (2007). The Golgi-associated protein GRASP is required for unconventional protein secretion during development. Cell *130*, 524–534.

Koh, Y.H., Popova, E., Thomas, U., Griffith, L.C., and Budnik, V. (1999). Regulation of DLG localization at synapses by CaMKII-dependent phosphorylation. Cell *98*, 353–363.

Kondylis, V., Tang, Y., Fuchs, F., Boutros, M., and Rabouille, C. (2011). Identification of ER proteins involved in the functional organisation of the early secretory pathway in *Drosophila* cells by a targeted RNAi screen. PLoS One *6*, e17173.

Krahmer, N., Hilger, M., Kory, N., Wilfling, F., Stoehr, G., Mann, M., Farese, R.V., Jr., and Walther, T.C. (2013). Protein correlation profiles identify lipid droplet proteins with high confidence. Mol. Cell. Proteomics *12*, 1115–1126.

Lazareva, A.A., Roman, G., Mattox, W., Hardin, P.E., and Dauwalder, B. (2007). A role for the adult fat body in *Drosophila* male courtship behavior. PLoS Genet. *3*, e16.

Lee, J.R., Urban, S., Garvey, C.F., and Freeman, M. (2001). Regulated intracellular ligand transport and proteolysis control EGF signal activation in *Drosophila*. Cell *107*, 161–171.

Lee, M.J., and Fried, S.K. (2006). Multilevel regulation of leptin storage, turnover, and secretion by feeding and insulin in rat adipose tissue. J. Lipid Res. *47*, 1984–1993.

Lee, M.J., Wang, Y., Ricci, M.R., Sullivan, S., Russell, C.D., and Fried, S.K. (2007). Acute and chronic regulation of leptin synthesis, storage, and secretion by insulin and dexamethasone in human adipose tissue. Am. J. Physiol. Endocrinol. Metab. *292*, E858–E864.

Lippincott-Schwartz, J., Yuan, L.C., Bonifacino, J.S., and Klausner, R.D. (1989). Rapid redistribution of Golgi proteins into the ER in cells treated with brefeldin A: evidence for membrane cycling from Golgi to ER. Cell *56*, 801–813.

Maley, F., Trimble, R.B., Tarentino, A.L., and Plummer, T.H., Jr. (1989). Characterization of glycoproteins and their associated oligosaccharides through the use of endoglycosidases. Anal. Biochem. *180*, 195–204.

Manjithaya, R., Anjard, C., Loomis, W.F., and Subramani, S. (2010). Unconventional secretion of *Pichia pastoris* Acb1 is dependent on GRASP protein, peroxisomal functions, and autophagosome formation. J. Cell Biol. *188*, 537–546.

Marra, P., Maffucci, T., Daniele, T., Tullio, G.D., Ikehara, Y., Chan, E.K., Luini, A., Beznoussenko, G., Mironov, A., and De Matteis, M.A. (2001). The GM130 and GRASP65 Golgi proteins cycle through and define a subdomain of the intermediate compartment. Nat. Cell Biol. *3*, 1101–1113.

Montague, C.T., Farooqi, I.S., Whitehead, J.P., Soos, M.A., Rau, H., Wareham, N.J., Sewter, C.P., Digby, J.E., Mohammed, S.N., Hurst, J.A., et al. (1997). Congenital leptin deficiency is associated with severe early-onset obesity in humans. Nature *387*, 903–908.

Moraru, A., Cakan-Akdogan, G., Strassburger, K., Males, M., Mueller, S., Jabs, M., Muelleder, M., Frejno, M., Braeckman, B.P., Ralser, M., et al. (2017). THADA regulates the organismal balance between energy storage and heat production. Dev. Cell *41*, 450.

Morton, G.J., Cummings, D.E., Baskin, D.G., Barsh, G.S., and Schwartz, M.W. (2006). Central nervous system control of food intake and body weight. Nature *443*, 289–295.

Nallamsetty, S., Austin, B.P., Penrose, K.J., and Waugh, D.S. (2005). Gateway vectors for the production of combinatorially-tagged His6-MBP fusion proteins in the cytoplasm and periplasm of *Escherichia coli*. Protein Sci. *14*, 2964–2971.

Neumuller, R.A., Wirtz-Peitz, F., Lee, S., Kwon, Y., Buckner, M., Hoskins, R.A., Venken, K.J., Bellen, H.J., Mohr, S.E., and Perrimon, N. (2012). Stringent analysis of gene function and protein-protein interactions using fluorescently tagged genes. Genetics *190*, 931–940.

Ozcan, L., Cristina de Souza, J., Harari, A.A., Backs, J., Olson, E.N., and Tabas, I. (2013). Activation of calcium/calmodulin-dependent protein kinase II in obesity mediates suppression of hepatic insulin signaling. Cell Metab. *18*, 803–815.

Ozcan, L., Wong, C.C., Li, G., Xu, T., Pajvani, U., Park, S.K., Wronska, A., Chen, B.X., Marks, A.R., Fukamizu, A., et al. (2012). Calcium signaling through CaMKII regulates hepatic glucose production in fasting and obesity. Cell Metab. *15*, 739–751.

Pfeiffer, B.D., Ngo, T.T., Hibbard, K.L., Murphy, C., Jenett, A., Truman, J.W., and Rubin, G.M. (2010). Refinement of tools for targeted gene expression in *Drosophila*. Genetics *186*, 735–755.

Rajan, A., and Perrimon, N. (2012). *Drosophila* cytokine unpaired 2 regulates physiological homeostasis by remotely controlling insulin secretion. Cell *151*, 123–137.

Ren, X., Sun, J., Housden, B.E., Hu, Y., Roesel, C., Lin, S., Liu, L.P., Yang, Z., Mao, D., Sun, L., et al. (2013). Optimized gene editing technology for *Drosophila* melanogaster using germ line-specific Cas9. Proc. Natl. Acad. Sci. USA *110*, 19012–19017.

Roh, C., Thoidis, G., Farmer, S.R., and Kandror, K.V. (2000). Identification and characterization of leptin-containing intracellular compartment in rat adipose cells. Am. J. Physiol. Endocrinol. Metab. *279*, E893–E899.

Scherer, P.E., Williams, S., Fogliano, M., Baldini, G., and Lodish, H.F. (1995). A novel serum protein similar to C1q, produced exclusively in adipocytes. J. Biol. Chem. *270*, 26746–26749.

Schindelin, J., Arganda-Carreras, I., Frise, E., Kaynig, V., Longair, M., Pietzsch, T., Preibisch, S., Rueden, C., Saalfeld, S., Schmid, B., et al. (2012). Fiji: an open-source platform for biological-image analysis. Nat. Methods *9*, 676–682.

Schotman, H., Karhinen, L., and Rabouille, C. (2008). dGRASP-mediated noncanonical integrin secretion is required for *Drosophila* epithelial remodeling. Dev. Cell *14*, 171–182.

Schuster, C.M., Davis, G.W., Fetter, R.D., and Goodman, C.S. (1996). Genetic dissection of structural and functional components of synaptic plasticity. I. Fasciclin II controls synaptic stabilization and growth. Neuron *17*, 641–654.

Soni, K.G., Mardones, G.A., Sougrat, R., Smirnova, E., Jackson, C.L., and Bonifacino, J.S. (2009). Coatomer-dependent protein delivery to lipid droplets. J. Cell Sci. *122*, 1834–1841.

Subramanian, M., Metya, S.K., Sadaf, S., Kumar, S., Schwudke, D., and Hasan, G. (2013). Altered lipid homeostasis in *Drosophila* InsP3 receptor mutants leads to obesity and hyperphagia. Dis. Model. Mech. *6*, 734–744.

Tennessen, J.M., Barry, W.E., Cox, J., and Thummel, C.S. (2014). Methods for studying metabolism in *Drosophila*. Methods *68*, 105–115.

Trayhurn, P., and Beattie, J.H. (2001). Physiological role of adipose tissue: white adipose tissue as an endocrine and secretory organ. Proc. Nutr. Soc. *60*, 329–339.

Tveit, H., Akslen, L.K., Fagereng, G.L., Tranulis, M.A., and Prydz, K. (2009). A secretory Golgi bypass route to the apical surface domain of epithelial MDCK cells. Traffic *10*, 1685–1695.

Veenendaal, T., Jarvela, T., Grieve, A.G., van Es, J.H., Linstedt, A.D., and Rabouille, C. (2014). GRASP65 controls the cis Golgi integrity in vivo. Biol. Open *3*, 431–443.

Walther, T.C., and Farese, R.V., Jr. (2012). Lipid droplets and cellular lipid metabolism. Annu. Rev. Biochem. *81*, 687–714.

Wang, Y., Li, G., Goode, J., Paz, J.C., Ouyang, K., Screaton, R., Fischer, W.H., Chen, J., Tabas, I., and Montminy, M. (2012). Inositol-1,4,5-trisphosphate receptor regulates hepatic gluconeogenesis in fasting and diabetes. Nature *485*, 128–132.

Wang, Y., Satoh, A., and Warren, G. (2005). Mapping the functional domains of the Golgi stacking factor GRASP65. J. Biol. Chem. *280*, 4921–4928.

Wright, V.M., Vogt, K.L., Smythe, E., and Zeidler, M.P. (2011). Differential activities of the *Drosophila* JAK/STAT pathway ligands Upd, Upd2 and Upd3. Cell. Signal. *23*, 920–927.

Wu, Q., Zhang, Y., Xu, J., and Shen, P. (2005). Regulation of hunger-driven behaviors by neural ribosomal S6 kinase in *Drosophila*. Proc. Natl. Acad. Sci. USA *102*, 13289–13294.

Xiang, Y., and Wang, Y. (2010). GRASP55 and GRASP65 play complementary and essential roles in Golgi cisternal stacking. J. Cell Biol. *188*, 237–251.

Yoshimura, S., Yoshioka, K., Barr, F.A., Lowe, M., Nakayama, K., Ohkuma, S., and Nakamura, N. (2005). Convergence of cell cycle regulation and growth factor signals on GRASP65. J. Biol. Chem. *280*, 23048–23056.

Zartman, J., Restrepo, S., and Basler, K. (2013). A high-throughput template for optimizing *Drosophila* organ culture with response-surface methods. Development *140*, 667–674.

Zhang, H., Liu, J., Li, C.R., Momen, B., Kohanski, R.A., and Pick, L. (2009). Deletion of *Drosophila* insulin-like peptides causes growth defects and metabolic abnormalities. Proc. Natl. Acad. Sci. USA *106*, 19617–19622.

Zhang, Y., Proenca, R., Maffei, M., Barone, M., Leopold, L., and Friedman, J.M. (1994). Positional cloning of the mouse obese gene and its human homologue. Nature *372*, 425–432.

STAR★METHODS

KEY RESOURCES TABLE

REAGENT or RESOURCE	SOURCE	IDENTIFIER
Antibodies		
GFP-nAb Agarose	Allele Biotech	ABP-nAb-GFPA050
Chicken anti-GFP	Abcam	ab13970
GFP coating antibody for ELISA	Allele Biotech	ACT-CM-GFPTRAP
GFP detection antibody for ELISA	Rockland	600-401-215
Rabbit anti-GRASP65	Abcam	ab30315
Anti-phospho-Threnonine	Cell Signaling	9381
Rabbit-anti-Lsp1-gamma	(Burmester et al., 1999)	N/A
Mouse monoclonal Anti-α-Tubulin	Sigma	T5168
Rabbit-anti-PLIN1	(Beller et al., 2010)	N/A
Rabbit-anti-tRFP	Evrogen	AB233
Rabbit-anti-Dilp5	(Geminard et al., 2009)	N/A
Bacterial and Virus Strains		
BL21(DE3)pLysS	EMD Millipore	69451-3
NEB 10-beta Competent E. coli	NEB	C3019H
Chemicals, Peptides, and Recombinant Proteins		
U73122	Tocris	1268
U73343	Tocris	4133
Brefeldin A1	Sigma	B5936-200UL
BAPTA-AM	Sigma	A1076-25MG
Ionomycin	Sigma	I9657-1MG
KN93	Santa Cruz Biotech	sc-202199
KN92	Santa Cruz Biotech	sc-311369
Effectene	QIAGEN	301427
Gibco Schneider's Drosophila Sterile Medium	ThermoFisher	21720024
SlowFade Gold antifade reagent with DAPI	Invitrogen	S36938
M3RM medium also known as Cl.8	(Zartman et al., 2013)	N/A
Fetal Bovine Serum	ThermoFisher	10437028
Gibco Penicillin-Streptomycin (5,000 U/mL)	ThermoFisher	15-070-063
Low melting agarose	Invitrogen	16520-100
Activated recombinant CaMKII	NEB	P6060S
Glycerol standard	Sigma	G7793-5ML
Free glycerol Reagent	Sigma	F6428-40ML
Triglyceride reagent	Sigma	T2449-10ML
Recombinant GFP protein	Vector Labs	MB-0752
Ni-NTA His•Bind Superflow Resin	EMD Millipore	70691-3
Recombinant 6XHis-MBP-*Drosophila* GRASP protein	This paper	N/A
Gateway LR Clonase II Enzyme mix	Invitrogen	11791-020
Gateway BP Clonase II Enzyme mix	Invitrogen	11789-020
MEGAscript T7 Transcription Kit	ThermoFisher	AMB1334-5
Q5 Site-Directed Mutagenesis Kit	NEB	E0554S

(*Continued on next page*)

Continued

REAGENT or RESOURCE	SOURCE	IDENTIFIER
Critical Commercial Assays		
1-step Ultra-TMB ELISA substrate	Pierce	34028
Renilla-Glo Luciferase reagent	Promega	E2710
Pro-Q Diamond Phosphoprotein Blot Stain	Thermo Fisher Scientific Inc	P33356
Experimental Models: Cell Lines		
D. melanogaster: Cell line S2R+	Laboratory of Norbert Perrimon	N/A
Experimental Models: Organisms/Strains		
UAS-GRASP::GFP	BDSC	8507, 8508
UAS-myr::GFP	BDSC	32197
UAS-Golgi-RFP	BDSC	30908
Lpp-Gal4	(Brankatschk and Eaton, 2010)	N/A
Df(3L)BSC552	BDSC	26502
Df(3L)BSC445	BDSC	24949
GRASP-RNAi	TRiP. This paper.	SH08449
GRASP-RNAi	TRiP. This paper.	SH08450
GRASP-RNAi	TRiP. This paper.	SH08451
IP3R-RNAi	BDSC/TRiP	JF01957
IP3R-RNAi	BDSC/TRiP	HMC03228
AkhR-RNAi	BDSC/TRiP	JF03256
Luciferase-RNAi	BDSC/TRiP	JF01355
GFP-RNAi	BDSC/TRiP	HMS00314
Dilp2-Gal4	(Wu et al., 2005)	N/A
UAS-Luciferase	(Rajan and Perrimon, 2012)	N/A
Lsp-Gal4	(Lazareva et al., 2007)	N/A
UAS-TrpA1	BDSC	26263
Mhc-Gal4	(Schuster et al., 1996)	N/A
UAS-GRASP::GFP	This paper	N/A
UAS-GRASP::GFP-CaMKII TtoD	This paper	N/A
UAS-GRASP::tagRFP-T	This paper	N/A
UAS-upd2::tagRFP-T	This paper	N/A
GRASP-del	This paper	N/A
Recombinant DNA		
pAc-upd2::GFP	(Hombria et al., 2005)	N/A
pACRenilla::Luciferase	Laboratory of Norbert Perrimon	N/A
pRmHa3 Spitz-GFP	(Lee et al., 2001)	N/A
GRASP cDNA	DGRC	BAC13N10
pDEST-HisMBP	Addgene	11085
pENTR-hLeptin	(Rajan and Perrimon, 2012)	N/A
Oligonucleotides		
GRASP-CH-1 (amplicon- forward primer with T7 promoter)	Designed by DRSC for this paper; Synthesized by IDT.	TAATACGACTCACTATAGGGGC CTCGATCAGGACAATGAT
GRASP-CH-1 (amplicon- reverse primer with T7 promoter)	Designed by DRSC for this paper; Synthesized by IDT.	TAATACGACTCACTATAGGGGA ACAGGTCGTCGTTCTCGT
GRASP-CH-2 (amplicon- forward primer with T7 promoter)	Designed by DRSC for this paper; Synthesized by IDT.	TAATACGACTCACTATAGGGCAG TACGCAGCAAAACGCTA
GRASP-CH-2 (amplicon- reverse primer with T7 promoter)	Designed by DRSC for this paper; Synthesized by IDT.	TAATACGACTCACTATAGGGGT CCGGATAGTTCGTCGTTG
GRASP_CKII_T270D_F	Q5-Site directed mutagenesis. This paper. Synthesized by IDT.	caccggcacTATTGAGCCACCGGCACAG

(*Continued on next page*)

Continued

REAGENT or RESOURCE	SOURCE	IDENTIFIER
GRASP_CKII_T270D_R	Q5-Site directed mutagenesis. This paper. Synthesized by IDT.	gctcaatatcCGGTGGTCTGACCTCGGC
GRASP_CKII_T83D_F	Q5-Site directed mutagenesis. This paper. Synthesized by IDT.	tacaCCTTACACCGAGCAACAAC
GRASP_CKII_T83D_R	Q5-Site directed mutagenesis. This paper. Synthesized by IDT.	aggtcCAGTTCGCGGACCGTCTG
Software and Algorithms		
ZenLite 2012	Zeiss	N/A
imageJ/FIJI	(Schindelin et al., 2012)	N/A
WEKA machine learning tool	http://fiji.sc/Trainable_Weka_Segmentation	N/A
Other		
Semi quantitative Mass Spectrometry Data	This Paper	S3C

CONTACT FOR REAGENT AND RESOURCE SHARING

Further information and requests for resources and reagents should be directed to and will be fulfilled by the Lead Contact, Akhila Rajan (akhila@fredhutch.org).

EXPERIMENTAL MODEL AND SUBJECT DETAILS

Experimental Animals

Species: Drosophila melanogaster

Only males were used in experiments at an age of 7-15 days post-eclosion.

For the RNAi experiments, crosses were maintained at 25C for 3 days, after which the progeny were shifted to 27C.

Flies were cultured in a humidified incubator at 25C on standard lab food containing per liter: 15 g yeast, 8.6 g soy flour, 63 g corn flour, 5g agar, 5g malt, 74 mL corn syrup.

Fly strains used in this study were from previous work (Rajan and Perrimon, 2012) and/or obtained from the Bloomington *Drosophila* stock center (BDSC): *UAS-GRASP::GFP* (BSDC# 8507, 8508), *UAS-myr::GFP* (BDSC#32197), *UAS-Golgi-RFP* (BDSC# 30908), *Lpp-Gal4* (Brankatschk and Eaton, 2010), *Mhc-Gal4* (Schuster et al., 1996), *Df(3L)BSC552* (BDSC# 26502), *Df(3L) BSC445* (BDSC# 24949). The following Transgenic RNAi Project (TRiP) lines were used: *IP3R-RNAi* (JF01957), *IP3R-RNAi* (HMC03228), *AkhR-RNAi* (JF03256), *Luciferase-RNAi* (JF01355), and *GFP-RNAi* (HMS00314). In addition, three independent GRASP RNAi lines, *SH08449, SH08450* and *SH08451,* were generated by the TRiP. qPCR analyses showed that GRASP knockdown is >75% for all three lines. Finally, the following UAS lines were generated: *UAS-GRASP::GFP, UAS-GRASP::GFP-CaMKII TtoD, UAS-GRASP::tagRFP-T, UAS-upd2::tagRFP-T.*

Cell Lines

Drosophila S2R+ cells were used for all cell culture related experiments. This cell line was chosen because previous studies have validated their applicability to study LD biogenesis (Guo et al., 2008) and protein secretion (Bard et al., 2006). The cells were maintained in Schneider's medium (GIBCO), 10% heat-inactivated FBS (SIGMA) and 5% Pen-Strep (GIBCO) at 25°C.

METHOD DETAILS

Tissue Culture

The day before transfection, cells were passaged to 60-80% confluency. For transfections related to ELISA experiments, cells were cultured in 96 well plates. They were transfected with 20ng/well *pAc-upd2::GFP* (Hombria et al., 2005), 10ng/well *pACRenilla::Luciferase*, and 150ng of dsRNA/well for knockdown experiments. Transfections were done using the Effectene kit (Cat# 301427, QIAGEN) as per the manufacturer's instructions.

dsRNA Production and Cell Treatments

Amplicons for dsRNAs were obtained from the *Drosophila* RNAi screening center (DRSC) and in vitro transcribed (IVT) using MEGAscript T7 Transcription Kit (Cat# AMB1334-5, ThermoFisher). IVT reactions were carried out as per the protocol provided by the DRSC (available at: http://www.flyrnai.org/DRSC-PRS.html). Amplicons used in this study are: *GRASP* (DRSC28969 and

see below), *dStim* (DRSC20158), *Syntaxin-5* (DRSC03432 and DRSC30696), *Rab2* (DRSC05017 and DRSC31649), *LacZ* dsRNA and *eGFP* dsRNA were used as controls. For *GRASP*, we designed two additional dsRNA amplicons, *GRASP-CH-1* and *GRASP-CH-2*. Details of primers used for generating these amplicons are provided in Oligonucleotide section of Key Resources Table. Except for *dStim*, all dsRNA knockdown experiments were carried out using a dsRNA pool of 2 or more independent dsRNAs per gene. We found that this produced a knockdown efficiency of >85% (based on qPCR analysis) in S2R+ cells. S2R+ transfected with dsRNAs were incubated for 4 days to allow for gene knockdown. On the 4th day, media was changed and the ELISA assay was carried out on the 5th day. Note the data is represented as percent change in Upd2/Leptin secretion normalized to transfection efficiency with 0% change indicating baseline level of secretion. See ELISA Assays procedure below.

Treatment of Cells with Drugs

For drug treatment experiments, the media was replaced with media containing the drug on day 3 after transfection with *upd2::GFP*. 18 hours later the conditioned media was used for ELISA, except for Ionomycin for which the treatment was done for 2-4 hours as increased exposure times caused cell death. Drugs used in this study for ELISA treatment include Brefeldin A1 (Cat# B5936-200UL, Sigma), BAPTA-AM (A1076-25MG, Sigma), Ionomycin (Cat#I9657-1MG, Sigma), KN93 (Cat#sc-202199, Santa Cruz), and U73122(Cat#1268, Tocris). Stock solutions of the drugs were made in DMSO as per the manufacturer's instructions, and used at a working concentration indicated in the figure legends of each experiment. DMSO treated replicates were used as controls. Note the data is represented as percent change in Upd2/Leptin secretion normalized to transfection efficiency, with 0% change indicating baseline level of secretion. See ELISA Assays procedure below.

ELISA Assays

GFP sandwich ELISA assay was used for detecting Upd2::GFP. On day 1, 96 well medium bind polystyrene plates (Cat#CLS3368-100EA, Sigma) were incubated overnight at 4C with coating antibody (Cat# ACT-CM-GFPTRAP, Allele Biotechnology) diluted in 0.01M pH8.0 bicarbonate buffer at a concentration of 1 μg/ml. On day 2, plates were washed briefly with PBS, blocked for 30 minutes with 1% BSA block in PBS, and coated with conditioned media and incubated overnight at 4C. Recombinant GFP protein (Cat# MB-0752, Vector labs), diluted in S2R+ cell growth media (64ng/ml to 4 ng/ml), was used in every ELISA plate as positive control to ensure linearity of GFP readings. On day 3, the plates were washed with PBS+0.05% Tween-20 (PBS-T), blocked with 1% BSA in PBS for 30 minutes at RT. GFP detection antibody (Cat# 600-401-215, Rockland) diluted 1:1000 in 0.1% BSA in PBS-T. Plates were washed with PBS-T and incubated with secondary HRP conjugated anti Rabbit secondary antibodies (Cat# ab136636, Abcam) diluted at 1:5000 in 1% BSA block. Plates were washed in PBS-T with a final wash in PBS. For detection, each well was incubated 100 μl 1-step Ultra-TMB ELISA substrate (Cat# 34028, Pierce), which was previously equilibrated to RT, for approximately 5-15 minutes until detectable blue colorimetric reaction occurred. Reaction was stopped with 2N sulphuric acid and absorbance was measured at 450nm. The TMB readings were normalized to transfection efficiency as measured from Renilla Luciferase assays (see below).

Renilla Luciferase Assay

On day 2 of the ELISA assay, after the conditioned medium was transferred for use in ELISA assays, cells were re-suspended in 50 μl of PBS, and incubated with 50 μl/well Renilla-Glo Luciferase reagent (Cat# E2710, Promega) for 10 minutes and read using a multiwell luminometer.

Endo H Sensitivity Assay

9 μl of protein, obtained by GFP-Immunoprecipitation (see below) from conditioned media of *upd2::GFP* transfected S2R+ cells, were digested with either Endo H(Cat# P0702S, NEB), PNGase F(Cat# P0704S, NEB), or Protein Deglycosylation Mix(Cat# P6039S, NEB) at 37C for 1 hour, as per NEB protocol. The digest was then and run on SDS-PAGE gel, and blotted to detect GFP. RNAaseB and Fetuin were used as positive controls for glycosidase reactions.

Cloning

All cloning was done using the Gateway Technology. Entry cDNA clones were PCR amplified from the appropriate templates [*GRASP* cDNA (from *BAC13N10*) and *upd2* cDNA (from plasmid *pAc-upd2GFP* (Hombria et al., 2005)] and cloned into pENTR-D/TOPO and pDONR221 using BP reaction (Gateway BP Clonase II enzyme mix, Cat#11789-020, Invitrogen). For human Leptin, the pENTR-hLeptin clone derived previously (Rajan and Perrimon, 2012) was used. For site directed mutagenesis of putative GRASP putative CaMKII sites, pENTR-GRASP was mutagenized using the Q5 Site-Directed Mutagenesis Kit from NEB (Cat # E0554S) to convert threonine encoding codons to aspartate. The sequence of oligonucleotides used for this mutagenesis reaction are provided in the Key Resources Table. The entry vectors were then moved using LR clonase reaction (Gateway LR Clonase II Enzyme mix, Cat#11791-020, Invitrogen) into destination vectors compatible with fly transformation, protein production, or cell culture and with the appropriate C-terminal tags.

Immunoprecipitation, Mass Spectrometry, and Western Blots

For Immunoprecipitation (IP) from S2R+ cells, protein for each condition was prepared by lysing 1 well of a 6-well dish, 4 days after transfection. For IP from fly fat bodies, GFP tagged GRASP was expressed using the LPP-Gal4 driver. 120 fed male flies or 150 starved male flies were harvested per replicate. Tissue was homogenized using 1mm zirconium beads (Cat#ZROB10, Next Advance) in Bullet Blender Tissue homogenizer (Model BBX24, Next Advance) in IP lysis buffer in the presence of protease inhibitors. 2 mg/ml was used per IP experiments performed with camelid antibodies GFP-nAb Agarose (Cat# ABP-nAb-GFPA050, Allele Biotech) as per the manufacturer's protocol. The sample was prepared for mass-spec as previously described (Neumuller et al., 2012). Western blots were performed as detailed in (Neumuller et al., 2012). Antibodies used include Chicken anti-GFP (Cat#ab13970, abcam) 1:2000 in TBS-0.05% tween-20 (TBS-T), Rabbit anti-GRASP65(Cat# ab30315,abcam) 1:10000 in 1% BSA block in TBS, Rabbit anti-Lsp1-gamma used at 1:10000 in milk block; as per directions in (Burmester et al., 1999) and monoclonal Anti-α-Tubulin 1:5000 in TBS-T(Cat# T5168, Sigma).

Recombinant Protein Expression

Full length GRASP was cloned into an *E.Coli* protein expression vector, pDEST-HisMBP, [gift of David Waugh (Addgene plasmid # 11085) (Nallamsetty et al., 2005)]. The plasmid was transformed into BL21DE3 pLysS strain of bacteria, 2 liter cultures were induced for 6 hours with 1M IPTG at 30°C. The 6XHis-MBP-GRASP protein was purified from bacterial lysates using Ni-NTA His•Bind Superflow Resin (EMD Millipore, 70691-3) to obtain purified recombinant 6x-His-MBP-GRASP (87kDA).

In vitro Kinase Assay and Phosphoprotein Blot Stains

For *in vitro* kinase assays, activated recombinant CaMKII (NEB, P6060S) was incubated with recombinant *Drosophila* GRASP for 60 minutes. We followed the kinase manufacturer's guidelines for setting up the kinase reaction. Briefly, the kinase was activated with Calmodulin, $CaCl_2$ and ATP for 10 minutes at 30°C. The activated kinase was incubated with the substrate for 30 minutes. The reaction was then run on a SDS-PAGE gel and Western blotted. The blot was probed with polyclonal antibodies that recognize phospho-Threonine (Cell Signaling, #9381) or with Pro-Q Diamond Phosphoprotein Blot Stain (Thermo Fisher Scientific Inc, P33356) as per the manufacturer's protocol.

TAG Assay

TAG assays were carried out as per the protocol described in (Tennessen et al., 2014). 3 adult male flies were used per biological replicates. Note that for adult TAG assays the most consistent results and lowest standard deviations were obtained using 10 days old male flies. The reagents used for assay were from Sigma Free glycerol (Cat # F6428-40ML), Triglyceride reagent (Cat# T2449-10ML) and Glycerol standard (Cat# G7793-5ML). It is critical that the triglyceride and free glycerol reagents are fresh. We used aliquots stored at -20C and never reused thawed reagents as reagents were unstable at 4C for longer than 2 days causing inconsistent readings. The TAG readings were normalized to total protein measured using BCA assay.

Generation of GRASP CRISPR Mutant

The gRNA sequence for GRASP65-A was designed using "DRSC find CRISPR (version 2)" (Housden et al., 2015). The GRASP65-A construct was generated by cloning annealed oligonucleotides encoding the gRNA sequence (TGTCCTGTACCTTGAGTACG) between the BbsI cut sites of the pl100 vector (Ren et al., 2013).

Nutrient Deprivation and Drug Feeding

Flies were cultured in a humidified incubator at 25C on standard lab food containing per liter: 15 g yeast, 8.6 g soy flour, 63 g corn flour, 5g agar, 5g malt, 74 mL corn syrup.

For nutrient deprivation experiments, 10 days old adult male flies were shifted to 1% sucrose agar for 5 days at 25C, after which they were used for experiments.

For drug feeding experiments, stock solutions for U73122 (Cat # 1268, Tocris) and control U73343 (Cat # 4133, Tocris) were dissolved first in chloroform and then in DMSO as per the manufacturer's instructions. The 5 mM DMSO stock was then added at a concentration of 10 μM to 1% sucrose in low melting agarose (Cat# 16520-100, Invitrogen). Flies were cultured in this condition for 4 days at 25C before they were used for imaging experiments.

Adult Brain Immunostaining

Immunostaining of adult brains were performed based on protocols from (Pfeiffer et al., 2010). Rabbit-anti-Dilp5 (Geminard et al., 2009) was used at a concentration of 1:800. Adult brains were dissected in PBS and fixed in cold 0.8% Para-formaldehyde (PFA) in PBS overnight at 4C. Tissues were washed the following day multiple times in 0.5% BSA and 0.5% Triton X-100 in PBS (PAT), pre-blocked in PAT+ 5% NDS for 2 hours at RT, and then incubated with the primary antibody overnight at 4C. The following day, the tissues were washed numerous times in PAT and then blocked again for 30 minutes in PAT+ 5% NDS and incubated in a cocktail with secondary antibodies (obtained from Jackson Immunoresearch) in block (final concentration of 1:500) 4 hours at room temperature. The samples were washed 3X-5X for 15 minutes per wash in PAT and mounted on slides with one layer of Scotch tape spacers in Slowfade gold antifade and imaged using Zeiss LSM 780 and 800 confocal systems.

Fat Body Preparation for Fixed Immunostaining and *Ex Vivo* Assays

As shown in Figure S5A, incisions, using dissection scissors (Cat# 500086, World Precision Instruments Inc), were made to release the ventral abdomen from the rest of the fly body. Flies used for dissection were adult males, 7-15 days old. Dissections were done in Ringer's medium (1.8 mM $CaCl_2$, 2 mM Kcl, 128 mM Nacl, 4 mM $MgCl_2$. 35 mM sucrose, 5 mM HEPES) and fixed in 4% formaldehyde for 20 minutes. They were rinsed with PBS and mounted in SlowFade Gold antifade reagent with DAPI (Cat# S36938, Invitrogen), with the cuticle side facing down.

For immunohistochemistry the fixed fat tissue was permeabilized in PBS+ 1.0% Triton-X-100 for 3X washes 5 minutes, subsequently washed with PBS+0.3% Triton-X-100 (Fat wash). Blocked for 30 minutes at room temperature (RT) with gentle agitation in Fat wash+5% Normal donkey serum (Block). Antibodies were diluted in block Rabbit-anti-PLIN1 (Beller et al., 2010)(1:1000); Chicken-anti-GFP (1:2000, Abcam, #ab13970); Rabbit-anti-tRFP (1:500, Evrogen, #AB233) and incubated overnight at 4C. Washed multiple times following day in fat wash at (RT) incubated with appropriate secondary antibody (from Jackson Immunoresearch) in block for 2-4 hours at RT. Washed 3X-5X for 5-15 minutes in fat wash, mounted in SlowFade Gold antifade reagent with DAPI (Cat# S36938, Invitrogen).

For live imaging and *ex vivo assays,* dissections were done in M3-based reference medium (M3RM medium also known as CI.8). For details on media prep refer to (Zartman et al., 2013). For *ex vivo* assays the dissected fat body explants were incubated with the appropriate drug, or DMSO control, for upto 30 minutes, followed by fixation in 4% formaldehyde for 20 minutes. They were rinsed with PBS and mounted in SlowFade Gold antifade reagent with DAPI. The following drugs were used in *ex*-vivo assays: KN93 (Cat# sc-202199, Santa Cruz Biotech) and its inactive analog KN92 (Cat# sc-311369, Santa Cruz Biotech) used at 100 nM.

QUANTIFICATION AND STATISTICAL ANALYSIS

Image Analysis Quantification

Image analysis was carried out in ZenLite 2012 and ImageJ (Schindelin et al., 2012). To calculate the intensity of Dilp and Upd2::tagRFP staining, mean gray value was calculated from maximum intensity projections of a similar number of confocal stacks using Image J.

We used the WEKA machine learning tool (http://fiji.sc/Trainable_Weka_Segmentation) to train datasets for classification of GRASP::GFP localization into 4 different categories. The training datasets were a collation of experiments from various conditions and fed into the tool as random Z-stacks and then trained. The trained classifier was then applied to control datasets and images were analyzed by eye to ensure that the classifier selected the right regions. The classifier was then applied in an unbiased manner to all experimental datasets. The classifier generated an image (as shown in S6B) that was then separated into different colors (yellow, violet, green, blue), by thresholding, followed by particle analysis to quantify the number of pixels per color. This was then represented as %area occupied by a particular compartment per XY slice, which was then averaged across the entire Z-stack.

ELISA

For ELISA assays, the ELISA signal readings are normalized to transfection efficiency; the data is represented as percent fold change from control used as baseline. Specifically, the ratio of TMB readings to Renilla Luciferase readings is calculated. This ratio from the control is used as a baseline and the data is represented as percent fold change of experimental conditions with respect to the control. Statistical significance quantified by Two-tailed t-test on 6 biological replicates per condition. Error bars represent %SD (Standard Deviation).

TAG Assays

For TAG assays, the TAG signal readings from whole fly lysate are normalized to total protein levels from BCA assay and/or the number of flies used per experiment. This normalized ratio from the control is used as a baseline and the data is represented as fold change of experimental genotypes with respect to the control. Statistical significance quantified by 2-tailed t-test on 3-6 biological replicates per condition. Error bars represent %SD (Standard Deviation).